Copyright

by

Heather Elizabeth Gilmer

1999

Evaluation of Fillet Weld Qualification Requirements

by

Heather Elizabeth Gilmer, B.A., M.A., B.S.

Thesis

Presented to the Faculty of the Graduate School
of the University of Texas at Austin
in Partial Fulfillment
of the Requirements
for the Degree of

Master of Science in Engineering

The University of Texas at Austin
August 1999

Evaluation of Fillet Weld Qualification Requirements

APPROVED BY

SUPERVISING COMMITTEE:

This thesis is dedicated to the memory of my grandfathers: to Wladyslaw Sandowski, who in 1995 hoped I knew what I was doing; and to Harrison Gilmer, who in 1994 was sorry I hadn’t grown up to be an engineer.

TABLE OF CONTENTS

CHAPTER 1: INTRODUCTION 1
- 1.1. Background 1
- 1.2. Scope of research 2
  - 1.2.1. Materials and fabrication 2
  - 1.2.2. Heat input 4
  - 1.2.3. Weld and base metal chemistry 5
  - 1.2.4. Welding method 8
  - 1.2.5. Test types 9
- 1.3. Statistical methods 11
- 1.4. Overview 12

CHAPTER 2: FILLET WELD SHEAR TEST 13
- 2.1. Fabrication 13
- 2.2. Testing and measurement 16
- 2.3. Results & Analysis 26
  - 2.3.1. Weathering consumables 26
  - 2.3.2. Non-weathering consumables 31
  - 2.3.3. Active flux 34
  - 2.3.4. Summary 35

CHAPTER 3: T-BEND TEST 41
- 3.1. Fabrication 41
- 3.2. Testing 45
- 3.3. Results and Analysis 49
  - 3.3.1. Weathering consumables 53
    - 3.3.1.1. Visual inspection 53
    - 3.3.1.2. Weld capacity 54
    - 3.3.1.3. Hardness 55

3.3.2. Non-weathering consumables 60
3.3.2.1. Visual inspection 63
3.3.2.2. Weld capacity 63
3.3.2.3. Hardness 66
3.3.3. Active flux 67
3.3.3.1. Visual inspection 69
3.3.3.2. Weld capacity 71
3.3.3.3. Hardness 71
3.3.4. Summary 73
CHAPTER 4: WELD ROOT CVN TEST 80
4.1. Fabrication 80
4.2. Testing 86
4.3. Results and Analysis 86
4.3.1. Effects of heat input and consumables 86
4.3.2. Effect of depth of V-notch into weld 95
CHAPTER 5: SUMMARY AND CONCLUSIONS 97
5.1. Evaluation of tests 97
5.1.1. Strength tests 97
5.1.2. T-bend test 98
5.1.3. Weld-Root CVN test 98
5.2. Welding consumables 99
5.3. Conclusion 99
APPENDIX 100
BIBLIOGRAPHY 107
VITA 108

ACKNOWLEDGEMENTS

I would like to thank the following people for their help and guidance: my advisor, Dr. Karl Frank; my second reader, Dr. Joseph Yura; the Ferguson Structural Engineering lab staff, Blake Stasney, Wayne Fontenot, Mike Bell, and Ray Madonna; Ronnie Medlock of the Texas Department of Tranportation; Haskell Ray of Trinity Industries; Ben Bristol, Buck Roberds, and John Mieske of PDM Bridge; J.R. Watson and the rest of the staff at the Applied Research Laboratories machine shop; Ken Miller, Trey Campbell, and Justin Billodeau; and Dr. Michael Engelhardt.

CHAPTER 1: INTRODUCTION

1.1. Background

The fillet weld qualification requirements in the current bridge welding code specifies that fillet welding procedures be qualified using a groove weld specimen (AWS D1.5-96, §5.10). Fillet welds have different properties from groove welds, however, so this test does not provide information about fillet weld characteristics. A typical small fillet weld will have more dilution of weld metal with base metal than the material at the center of a large groove weld, which is what is examined in the standard test. In addition, the groove weld microstructure will be refined in subsequent passes; fillet welds are typically single-pass. In practice, welding procedures that give good test results for a groove weld do not necessarily produce the best fillet welds. In particular, fabricators have reported that the heat input required to produce a groove weld specimen that will pass the specified tests is too high for many fillet welds. This is particularly problematic with T joints welded simultaneously on both sides, where the total heat input to the welded area is greatly increased. There are anecdotal reports that fillet welds made with procedures that pass the qualification tests have failed in the field.

One particular type of failure is described in Miller (1997). When two high-heat welds are made on opposite sides of a T joint with a relatively thin stem, the fusion zones of the two welds may join, forming a single region of molten metal that can develop a plane of weakness in the weld and crack as it cools.

In addition, many fabricators think that much of the testing is unnecessary. They feel that they are wasting time and money by conducting tests on procedures that have been tested repeatedly in the past and are expected to perform consistently in the future. In addition, some tests may not be necessary because the results may depend more on the quality of the welding materials than on the procedure, and so as long as the welding electrode manufacturers conduct appropriate tests of their materials, these properties need not be tested in the finished welds.

At the start of this study, a meeting was held with representatives from various state departments of transportation and other government agencies and members of the steel bridge and welding industries. Potential tests were suggested from among fillet weld tests the representatives had had experience with. A nationwide survey of fabricators was taken to determine current standard practice for web-to-flange and stiffener-to-web bridge welding procedures.

1.2. Scope of research

In this study, three types of test specimens were investigated as possible alternatives to AWS Test Plate A, shown in Figure 5.1 of AWS D1.5-96 and reproduced here as Figure 1.1. Test variables included welding consumables, heat inputs, and fabrication techniques (whether joints were welded one side at a time or simultaneously). One test also included web thickness as a variable.

1.2.1. Materials and fabrication

All specimens were welded using the submerged arc process by fabricators experienced with large fracture-critical bridges, and then machined and tested at the Ferguson Structural Engineering Laboratory. Electrode strengths were matched to the base metal.

Three sets of welding consumables were used: weathering (860/LA-75, 3/32” wire), non-weathering (960/L-61, 3/32” wire), and active flux (780/L-61, 5/64” wire). “Weathering” consumables are those that are appropriate for use

with weathering steel. The fabricator who provided the weathering specimens uses that electrode-flux combination for all its submerged-arc welding. The non-weathering and active flux specimens came from two different shops within the same company. The 960/L-61 combination is this company's standard for production welds. The active flux combination is what this company would prefer to use for fillet welds. Active fluxes contain deoxidizers to prevent porosity and cracking but are suited only for single-pass welds. Neutral fluxes are used for multiple-pass welding such as that required for the AWS standard test plate. Test plates welded using the 780/L-61 (active flux) combination often do not meet the Charpy V-Notch (CVN) toughness requirements of AWS D1.5-96 §5.19.5 even though the fabricators feel this choice of consumables is more appropriate for the fillet welds used in production.

The base metal for all specimens was specified as A709 Gr. 50 steel, although chemical analysis suggests that the base metal used with the active flux was weathering steel.

1.2.2. Heat input

Heat input is calculated using Equation 1.1, taken from AWS D1.5-96 §5.12.

$$\text{Heat Input (kJ/in)} = \frac{\text{Amperage} \times \text{Voltage} \times 0.6}{\text{Travel Speed (in/min)}} \tag{1.1}$$

Both high and low heat inputs were used in fabricating the test specimens. The high heat inputs were approximately 50 kJ/in and the low heat inputs were approximately 35 kJ/in. This range of heat inputs was determined from the survey of fabricators taken at the start of the project. The values chosen were near the bottom and top of the range of reported heat inputs but within normal expectations for what heat inputs might be used with the weathering and non-weathering consumables already in use. The welding procedure variables are listed in Table 1.1.

Table 1.1. Welding procedure variables

Consumables	Heat input classification	Current (A)	Voltage (V)	Travel speed (in/min)	Heat input (kJ/in)
Weathering	low	300	25	13	34.6
	high	400	30	15	48.5
Non-weathering	low	310	23	12	35.6
	high	360	28	12	50.4
Active flux	low	345	23	14	34.0
	high	430	34	18	48.7
Additional specimens, T test only					
Non-weathering	low	320	24	14	34.2
	high	400	28	14	48.0

1.2.3. Weld and base metal chemistry

Samples of the high and low heat weld metal for each set of consumables were sent to a laboratory for chemical analysis, along with samples from each size of plate stock used by each fabricator. The 3/4-in plate samples came from the Charpy impact blocks containing the weld samples, so there are two 3/4-in plate samples for each set of consumables. Sample 1 is from the specimen containing the low-heat weld, and Sample 2 is from the specimen with the high-heat weld. The chemical analyses of the weathering, non-weathering, and active-flux specimens are summarized in Tables 1.2, 1.3, and 1.4, respectively. The carbon equivalent, a measure of weldability, is given at the bottom of the table and is calculated using Equation 1.2, which is given in AWS D1.5-96 §5.4.2.

$$\mathrm{CE} = \mathrm{C} + \frac{\mathrm{Mn}}{6} + \frac{\mathrm{Cr} + \mathrm{Mo} + \mathrm{V}}{5} + \frac{\mathrm{Ni} + \mathrm{Cu}}{15} \qquad (1.2)$$

Table 1.2. Chemical analysis of materials used in "weathering" specimens (values reported in %)

Element	**Low heat weld metal**	**High heat weld metal**	**3/8-in plate**	**1/2-in plate**	**5/8-in plate**	**3/4-in plate, sample 1**	**3/4-in plate, sample 2**
Carbon	0.07	0.08	0.19	0.18	0.14	0.17	0.15
Manganese	1.52	1.36	0.98	1.14	1.15	1.15	1.23
Phosphorus	0.012	0.012	0.009	0.017	0.016	0.022	0.020
Sulfur	0.013	0.008	0.007	0.007	0.010	0.017	0.017
Silicon	0.57	0.47	0.20	0.27	0.19	0.29	0.30
Nickel	0.61	0.41	< 0.01	< 0.01	0.01	< 0.01	< 0.01
Chromium	0.03	0.03	0.02	0.03	0.04	0.04	0.04
Molybdenum	< 0.01	< 0.01	< 0.01	0.03	< 0.01	< 0.01	< 0.01
Copper	0.08	0.07	0.01	0.01	0.04	0.01	0.01
Vanadium	0.009	0.019	0.043	0.043	0.043	0.040	0.043
Titanium	0.008	< 0.005	< 0.005	< 0.005	< 0.005	< 0.005	< 0.005
Niobium	< 0.005	< 0.005	< 0.005	< 0.005	< 0.005	< 0.005	< 0.005
Aluminum	0.014	0.013	0.041	0.030	0.010	0.020	0.045
Boron	< 0.0005						
Nitrogen	0.0038	0.0046	0.0096	0.0069	0.0051	0.0050	0.0037
Carbon equivalent	0.38	0.35	0.37	0.39	0.35	0.38	0.37

Table 1.3. Chemical analysis of materials used in "non-weathering" specimens (values reported in %)

Element	Low heat weld metal	High heat weld metal	3/8-in plate	5/8-in plate	3/4-in plate, sample 1	¾-in plate, sample 2
Carbon	0.10	0.11	0.08	0.15	0.19	0.19
Manganese	1.60	1.42	1.09	0.99	1.20	1.14
Phosphorus	0.017	0.016	0.014	0.007	0.015	0.016
Sulfur	0.016	0.012	0.011	0.008	0.018	0.016
Silicon	0.51	0.35	0.20	0.24	0.26	0.26
Nickel	0.03	0.02	0.01	0.01	< 0.01	< 0.01
Chromium	0.04	0.04	0.03	0.02	0.04	0.04
Molybdenum	< 0.01	< 0.01	< 0.01	< 0.01	< 0.01	< 0.01
Copper	0.09	0.06	0.04	0.22	0.01	0.01
Vanadium	0.015	0.028	0.024	0.034	0.049	0.046
Titanium	< 0.005	< 0.005	< 0.005	< 0.005	< 0.005	< 0.005
Niobium	< 0.005	< 0.005	< 0.005	< 0.005	< 0.005	< 0.005
Aluminum	0.006	0.008	0.009	0.026	0.033	0.031
Boron	< 0.0005	< 0.0005	< 0.0005	< 0.0005	< 0.0005	< 0.0005
Nitrogen	0.0070	0.0075	0.0052	0.0104	0.0041	0.0045
Carbon equivalent	0.39	0.37	0.28	0.34	0.41	0.40

Table 1.4. Chemical analysis of materials used in “active flux” specimens (values reported in %)

Element	Low heat weld metal	High heat weld metal	3/8-in plate	1/2-in plate	5/8-in plate	3/4-in plate, sample 1	3/4-in plate, sample 2
Carbon	0.07	0.11	0.13	0.11	0.06	0.16	0.16
Manganese	1.16	1.69	1.00	0.93	1.08	1.26	1.21
Phosphorus	0.020	0.017	0.009	0.007	0.016	0.013	0.014
Sulfur	0.011	0.008	0.021	0.012	0.006	0.028	0.024
Silicon	0.76	0.65	0.32	0.23	0.38	0.36	0.36
Nickel	0.13	0.19	0.11	0.17	0.20	0.30	0.31
Chromium	0.23	0.36	0.49	0.42	0.54	0.58	0.58
Molybdenum	< 0.01	< 0.01	< 0.01	< 0.01	< 0.01	< 0.01	< 0.01
Copper	0.20	0.21	0.31	0.28	0.27	0.26	0.27
Vanadium	0.025	0.035	0.036	0.014	0.044	0.054	0.053
Titanium	0.035	0.023	< 0.005	< 0.005	< 0.005	< 0.005	< 0.005
Niobium	0.006	< 0.005	< 0.005	< 0.005	< 0.005	< 0.005	< 0.005
Aluminum	0.025	0.013	< 0.005	< 0.005	0.011	0.030	0.027
Boron	0.0008	0.0005	< 0.0005				
Nitrogen	0.0076	0.0090	0.0113	0.0086	0.0052	0.0078	0.0075
Carbon equivalent	0.34	0.50	0.43	0.38	0.39	0.53	0.53

The high nickel, chromium, and copper contents of the base metal used with the active flux welds are consistent with the chemical composition of weathering steel. All the other base metals were consistent with non-weathering steel.

1.2.4. Welding method

Some of the test specimens had fillet welds on opposite sides of a plate, similar to a stiffener-to-web or web-to-flange weld. The welds can be made one side at a time, or on both sides simultaneously using an opposing arc system such as a Dart Welder. The welds made on one side at a time will be referred to as single-sided and the welds made on both sides simultaneously (without offsetting the opposing electrodes from one another along the axis of the weld) will be referred to as dart-welded. Dart welding increases the total heat input to the welded area, so it should have a similar effect to that of higher heat input, unless the plate between the opposing arcs is thick enough to prevent their interaction.

1.2.5. Test types

All tests will be described in greater detail in following chapters. The three tests investigated will be referred to as the shear test, the T-bend test, and the Weld Root Charpy V-Notch test (WRCVN). The shear test is used to measure weld shear strength. The specimen is similar to the transverse shear strength specimen described in AWS B4.0-92 and is illustrated in Figure 1.2. Tension is applied to the ends of the specimen until a weld breaks or a plate yields. This particular shear test was chosen in part because it was possible to use dart welding to fabricate the specimens. It was hoped that the central 5/8-inch plate was thin enough to allow an effect from dart welding. To keep the plate thickness low, a weld size of 1/4 in was chosen, which was the smallest weld used by all fabricators surveyed. The 1/4-in size was used for all samples for all tests performed.

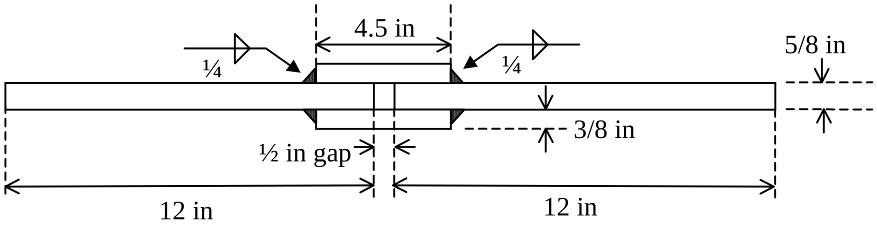

Figure 1.2. Fillet weld shear test specimen

The T-bend test is based on a test that has been used by the Georgia and California departments of transportation and has been utilized for high-performance steel fillet welds. The test gives an indication of weld ductility. Figure 1.3 is a schematic of the test setup. The specimen rests on the supports and tension is applied to the web of the T from below. Testing was continued until load capacity dropped or the notch in the specimen was closed. Specimens were fabricated using both dart and single-sided welds, and with two different web sizes.

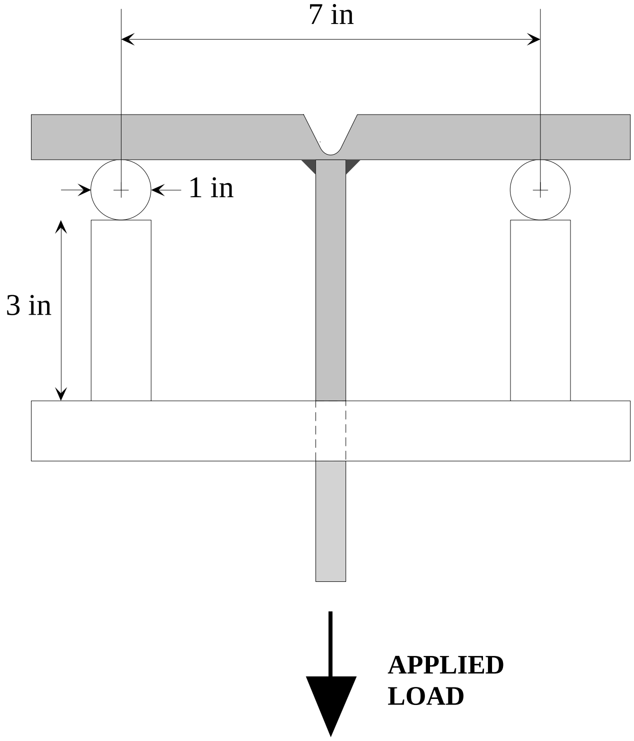

Figure 1.3. T-bend test setup

The WRCVN specimen is a modified Charpy V-notch (CVN) impact bar, based on a test specimen developed by Chris Hahin of the Illinois Department of Transportation and described in Hahin (1990). The V-notch in this specimen is cut at the root of a 60° groove weld which simulates a fillet weld, as shown in Figure 1.4a. The AWS standard calls for a notch located at the center of a large multiple-pass groove weld, as shown in Figure 1.4b, reproduced from AWS D1.5-96, Figure 5.1. The specimens are tested as per ASTM A370, “Charpy Impact Testing”.

The WRCVN specimen should provide a better representation of fillet properties than the AWS standard specimen would. The center of the AWS standard test weld bears no similarity to a fillet weld, while the root of the WRCVN 60° groove weld should have similar base metal dilution to that found in fillet welds. The groove weld is in essence a multiple-pass fillet weld.

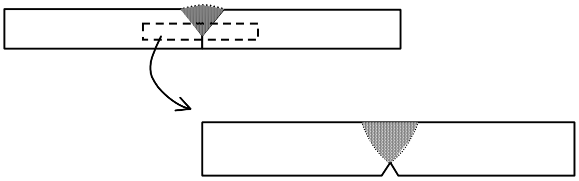

Figure 1.4a. Location of CVN impact bar within WRCVN plate

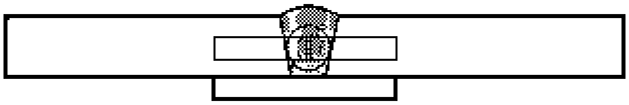

Figure 1.4b. Location of CVN impact bar within AWS standard plate

1.3. Statistical methods

An analysis of variance (ANOVA) was used with some sets of test results to determine the effects of heat input and welding method on strength and hardness. ANOVA is a statistical test that determines to what extent a difference between sample means is due to difference between the true population means and to variation within the samples (Devore and Peck, 1993). One diagnostic value that is obtained from such an analysis is the *p* value, which essentially is the probability that the difference between the samples is not due to a difference between the populations. For example, a difference of five units in two sample means is much more significant if the samples each fall within a range of only two units than if the samples each have a range of one hundred units. In the first case, the samples do not overlap and are clearly quite different. In the other case, the two samples overlap considerably. The *p* value is related to the confidence level in the significance of the difference between the samples. For instance, a $p = 0.02$ corresponds to a 98% confidence level. Usually a 95% confidence level is the standard for statistical significance. In a two-factor ANOVA, three effects are measured: the effects of the two factors, and any interaction between the factors.

1.4. Overview

Test welds were made with the three sets of consumables, two heat inputs, two welding methods where dart welding was possible, and two different web thicknesses in the T specimens. Tests were performed to determine shear strength, hardness, toughness, and T-joint behavior. At the end of this report, recommendations will be made regarding testing to evaluate fillet welds.

CHAPTER 2: FILLET WELD SHEAR TEST

2.1. Fabrication

The thicknesses of the plates in the fillet weld shear test specimens were chosen so that failure would be in the weld. For design purposes the effective throat was assumed to be 0.707 times the leg length of 0.25 in. This gives a weld throat area of $0.707 * 0.25 = 0.177$ in^2 per inch of weld length. A weld with a nominal tensile strength of 70 ksi and an estimated shear strength of $0.6 * 70 = 42$ ksi would then be able to support $0.177 * 42 = 7.4$ kips per inch of length, and the two welds together should support $7.4 * 2 = 14.8$ kips per inch of length. A 50-ksi yield strength steel would then require at least $14.8/50 = 0.3$ inches of thickness to equal or exceed the weld capacity. For the pull plates, 5/8-inch thick plates were chosen, double the required thickness. Each lap plate was 3/8 in thick. Load was assumed to be distributed equally between the two welds on either side of the plate.

Transverse welds are stronger than longitudinal welds. It is stated in the AISC LRFD Manual Part 8 that “[f]illet welds are approximately one-third stronger in the transverse direction than in the longitudinal direction” (p. 8-118), and there is an optional provision in LRFD Specification Appendix J2.4 that allows the calculated strength of a transverse fillet weld to be increased by 50%. In addition, in the case of submerged arc welding (SAW), the effective throat is defined in LRFD as equal to the leg size for small welds in order to account for the greater penetration achieved with this process. Both of these factors were neglected in the design, but the conservative design should have compensated for the effects of penetration and transverse loading. Nevertheless, some specimens yielded in the plates instead of breaking in the welds. Had the plates been thick enough to ensure failure in the welds, they might not have shown any dart welding effects.

The specimens were long enough to provide sufficient distance between the machine grips and the weld so that stress concentrations at the grips would not affect the failure of the specimen. Because the critical section of these specimens was in the welds, two inches away from the midpoint, the specimens were several inches longer than standard steel tensile coupons.

Four plates were made for each set of weld consumables. The variables were heat input and welding method. For each set of parameters, the fabricators prepared a single plate, from which the test specimens were cut. Figure 2.1 shows the dimensions of the test plate as welded. The plates were then saw-cut into strips 2 in wide as shown in Figure 2.2 and milled to a constant width of 1.75 in through the weld and lap-plate area. The end sections were not used. The finished dimensions are shown in Figure 2.3. Each test specimen was 24.5 in long.

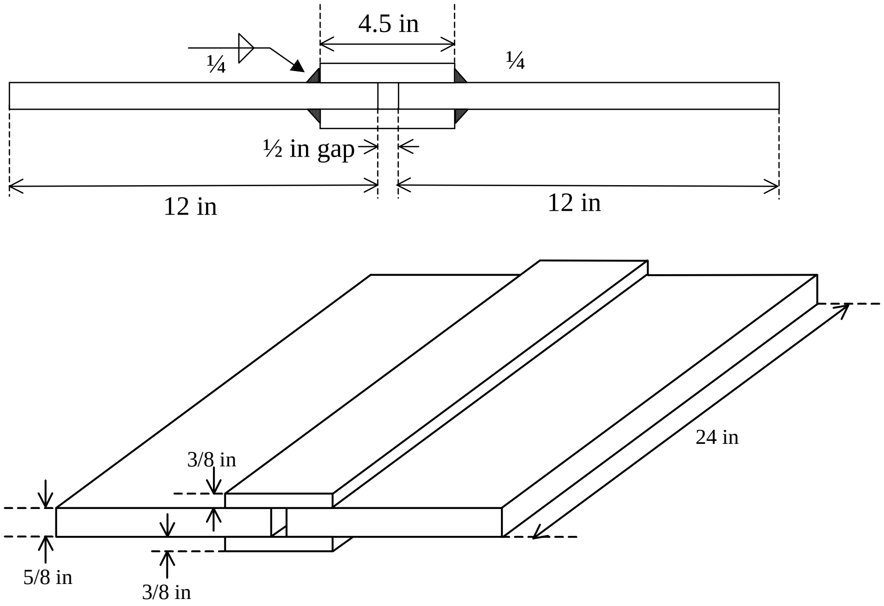

Figure 2.1: Shear test plate as fabricated

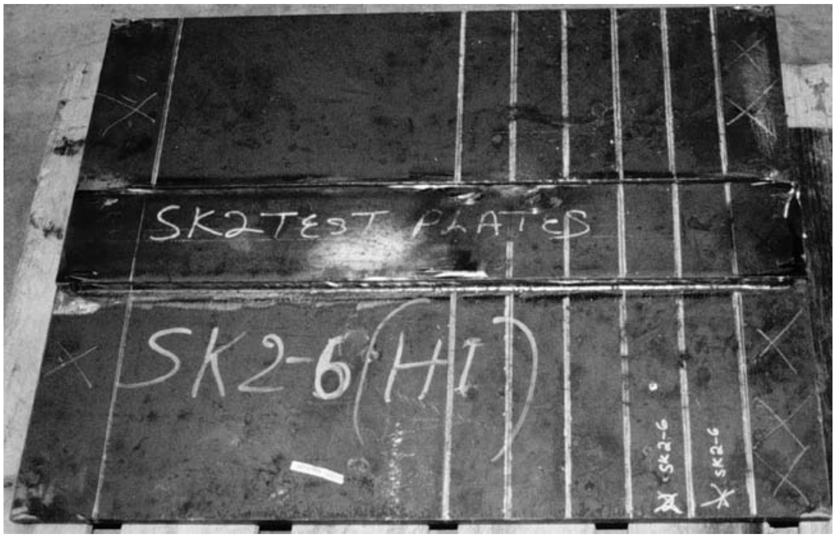

Figure 2.2: Strips marked on test plate

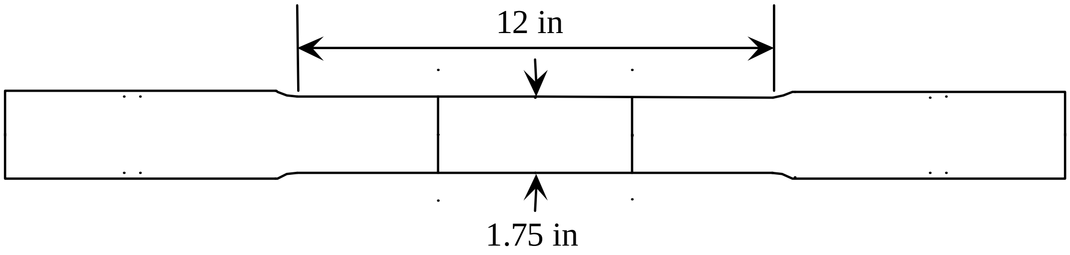

Figure 2.3: Dimensions of finished specimen

The dart-welded specimens were more difficult to fabricate because the plate had to be held upright and wing plates were required to hold the flux and to support the guide wheels of some welders. Figure 2.4 shows a plate tacked in an upright position with wing plates tacked on. Another fabricator clamped on angles in place of tacked wing plates.

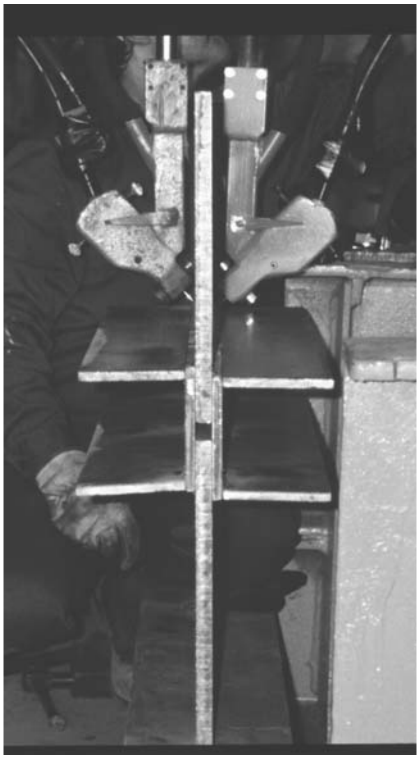

Figure 2.4: Test plate with tacked wing plates

2.2. Testing and measurement

The specimens were loaded at a constant deformation rate of 0.05 in/min. Loading continued until a weld broke or the load carried by the specimen dropped, indicating a reduction in area of the plate. Figure 2.5 shows a shear specimen in the test setup. Load and deformation (crosshead displacement) data were collected electronically. Figure 2.6 shows a closeup view of the break in a shear specimen after testing.

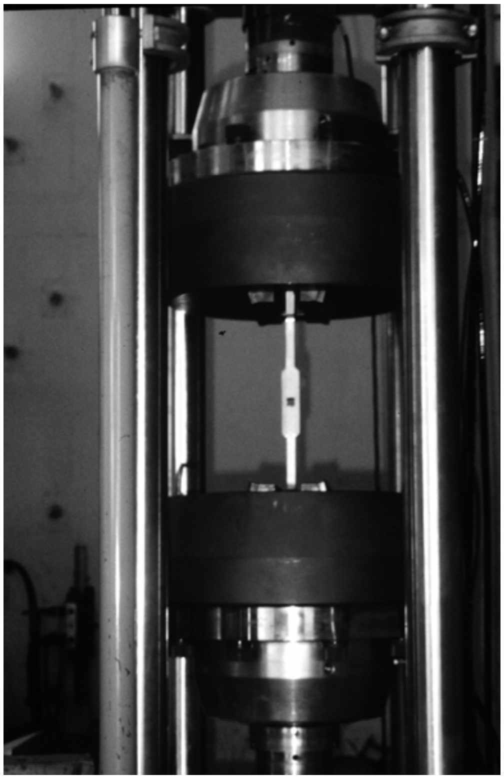

Figure 2.5: Shear test setup

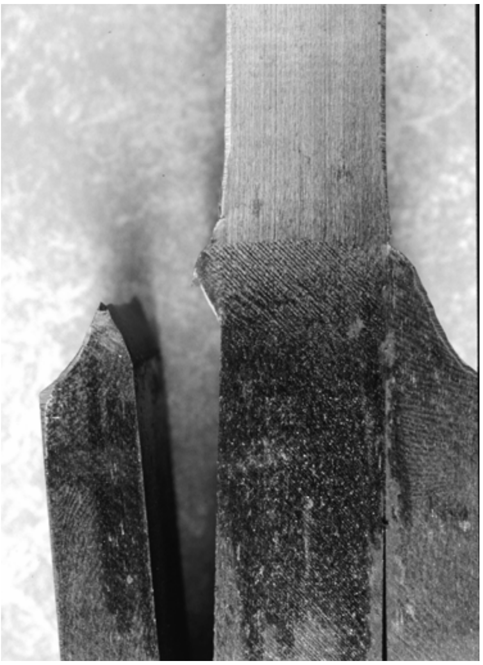

Figure 2.6: Failed weld in tested shear specimen

Stress rather than load was required for analysis of the results because the welds were not all exactly the same size. Calculating the weld stress required measuring the weld cross sections. Pieces were cut from untested portions of the plates; measurements of these sections were used to estimate weld size in the test welds. Each cross section was polished and etched. Figures 2.7a and 2.7b show typical cross sections. The specimens made with the weathering consumables had concave weld profiles like those in Figure 2.7a. The other two sets of specimens had convex weld profiles like those in Figure 2.7b. The dots in Figure 2.7b are the result of hardness testing.

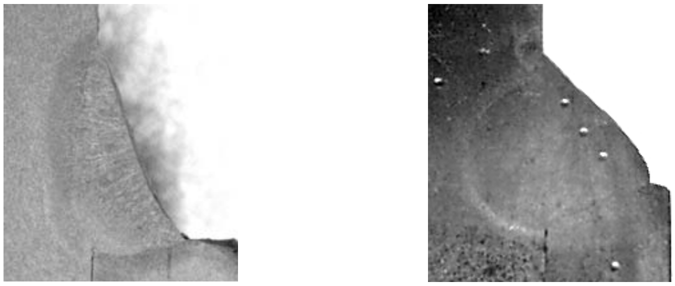

(a) **(b)**

Figure 2.7. Typical weld cross-sections, (a) convex and (b) concave

Schematic drawings of the two kinds of cross-section are shown in Figures 2.8a and 2.8b, adapted from AWS A3.0-94, Figures 25(A) and 25(B).

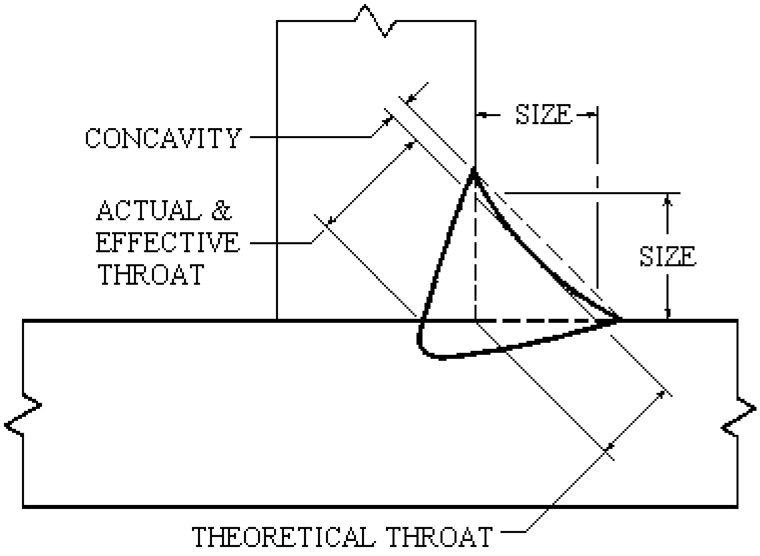
CONCAVITY
SIZE
ACTUAL &
EFFECTIVE
THROAT
SIZE
THEORETICAL THROAT

(a) concave weld profile

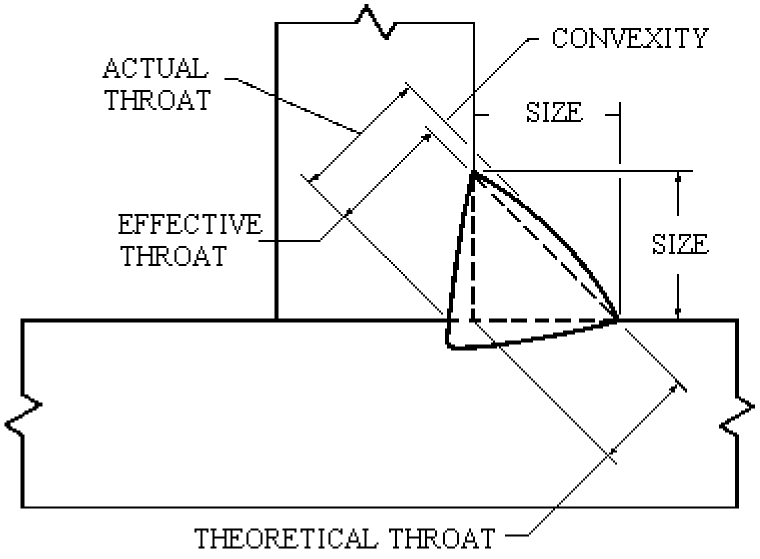
CONVEXITY
ACTUAL
THROAT
SIZE
EFFECTIVE
THROAT
SIZE
THEORETICAL THROAT

(b) convex weld profile

Figure 2.8. Characteristic dimensions of weld cross-sections

The effective area for calculating stress is the weld throat times the weld length or specimen width. Measuring the weld throat proved to be a very complicated matter. First, it was difficult to determine what the weld leg sizes should be for the concave welds. Annex I of AWS D1.5-96 defines the throat in terms of a line parallel to a line connecting the two weld toes, but falling entirely within the weld profile, as illustrated in Figure 2.8. Such a line was used to define the leg sizes for the concave welds in this study. However, it was not always obvious where this line should be drawn. In addition, once the lines were drawn, the measurements themselves were not very accurate. Dimensions could only be measured to the nearest 0.01 in, which is on the order of a 5% error for the 1/4-in welds.

Furthermore, it is not at all clear how the throat should be defined. Welds are assumed for design purposes to have equal legs, when in practice this may not be the case, as shown in Figure 2.7a. The assumption for effective throat size is that the throat is at a right angle to the weld surface (as defined by the toe-to-toe or parallel line shown on Figure 2.8), and that the entire tensile force is transmitted by shear on the effective area. However, when transverse fillet welds break in shear, the fracture surface is not perpendicular to the weld face, as was shown in Figure 2.6. Moreover, the shear force on the weld will depend on the angle of the fracture surface with respect to the direction of loading.

Miazga & Kennedy (1988) derive from equilibrium an equation for weld shear stress in terms of weld dimensions and the orientation of the weld with respect to the direction of load application. They assume that the leg sizes are equal. Equation 2.1 is derived from similar principles, but allows for differing leg sizes and assumes a transverse weld (see the appendix for the derivation).

$\tau = P(\cos\alpha - a\sin\alpha)/[Lh\sin\phi / \sin(\alpha + \phi)]$, (2.1)

where:

τ = shear stress on weld

P = load on weld

α = angle of fracture plane from loading direction

h = length of leg parallel to loading direction (“horizontal”)

v = length of leg perpendicular to loading direction (“vertical”)

a = stress distribution coefficient

    If $a = 0$, tensile force on “vertical” leg acts at weld root

    If $a = 1$, tensile force on “vertical” leg is uniformly distributed

L = length of weld, or width of specimen

ϕ = angle of weld face from loading direction; $v/h = \tan\phi$

    (ϕ concept from Kametkar (1982))

Figure 2.9 illustrates some of the dimensions used in Equation 2.1.

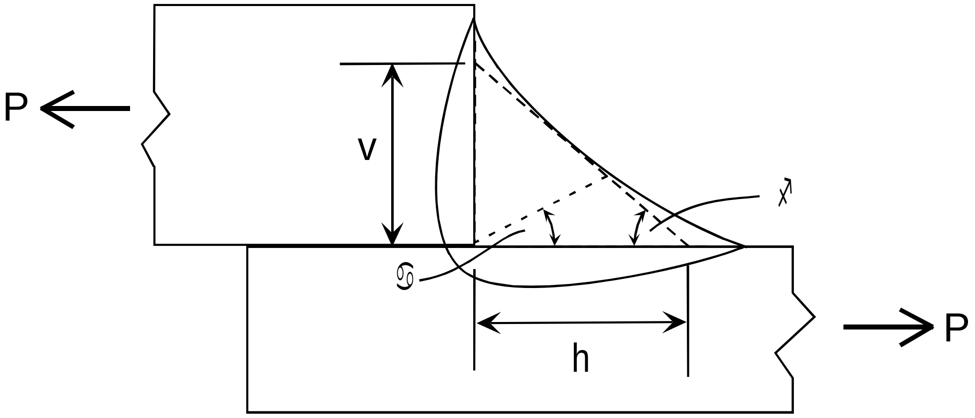

(a) concave weld profile

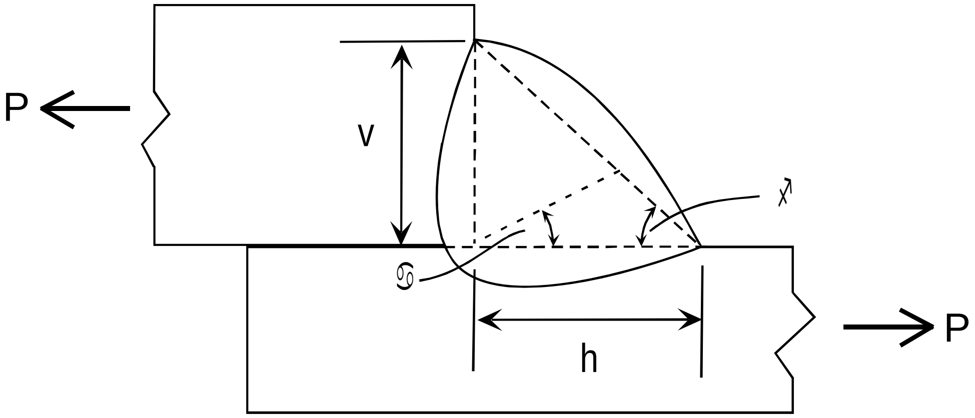

(b) convex weld profile

Figure 2.9. Dimensions and forces used to calculate shear stress

Figure 2.10 shows the effect of the constant *a*; *a* = 0 means the load acting at the “vertical” weld face (perpendicular to the direction of loading) is concentrated at the weld root, and *a* = 1 means the load is distributed evenly over the vertical weld face.

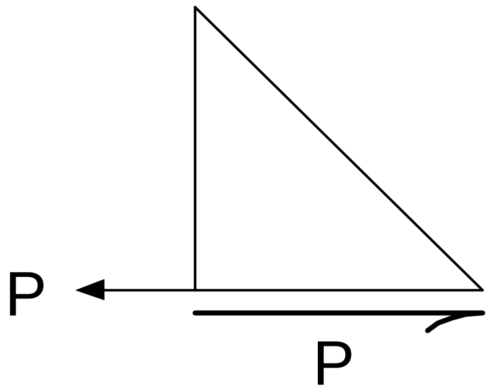

(a) ***a*** **= 0**

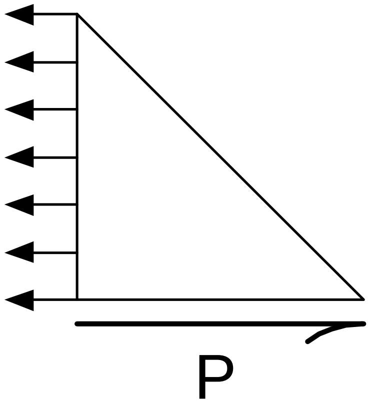

(b) ***a*** **= 1**

Figure 2.10. Load distribution constant *a*

The angle α at which τ reaches a maximum should be the failure angle. For $\alpha \leq 45°$, τ is highest for $a = 0$ and lowest for $a = 1$. If equal legs of length d ($h = v = d$), a fracture angle α of 45°, and $a = 0$ are all assumed, then Equation 2.1 gives shear stress $\tau = P/Ld$, where d is leg length, not throat. Under the standard design assumption, shear stress is calculated as P/Lx, where x is effective throat length. The throat is defined at a 45° angle to the legs, so shear stress is

$P/(Ld \sin 45°)$. It then appears that the standard assumption overestimates the shear stress by a factor of $1/\sin 45°$, or 1.41, even if it is appropriate to assume a fracture angle of 45°. However, for equal leg lengths and $a = 0$, shear stress τ reaches a maximum at a fracture angle α of 22.5°, not 45°. This is in fact much closer to actual weld fracture behavior, as was shown in Figure 2.6. For this smaller fracture angle, $\tau = P \cos 22.5° \sin 67.5°/(Ld \sin 45°) = P \cos^2 22.5°/(Ld \sin 45°)$. Under the standard assumption, shear stress is overestimated by a factor of $1/\cos^2 22.5°$, or 1.17. If the SAW provision for effective throat in LRFD is used, the shear stress is underestimated by a factor of $\sin 45°/\cos^2 22.5°$, or 0.83.

Miazga & Kennedy empirically determined that the value for the stress distribution factor a should be 0.345. However, their study had only equal-leg welds. They did not report weld process either in their own experiment or in the data from their literature survey, but the process was probably not SAW. There is no reason to assume that this value should be appropriate for unequal-leg welds or for different welding processes. Values of $a = 0$, 0.345, and 1 were considered in evaluating the data from this study. The best fit to of predicted to measured weld parameters (fracture surface angle and length) appears to be $a = 0$. Choosing $a = 0$ also gives the best correlation of weld strength to the weld hardness results. Therefore this value was used in all stress calculations. However, the difficulty in determining the value of a should be considered another source of uncertainty in the stress calculations. The size of the welds is an additional uncertainty.

As an example, consider a nominal 1/4-in weld of length $L = 1.702$ in, with leg sizes $h = 0.29$ in and $v = 0.33$ in, and carrying a load P of 35.2 kips. $\phi = \tan^{-1}(v/h) = 0.850$ rad. a is assumed to be zero. The value of α for which τ as calculated from Equation 2.1 is a maximum is 0.350 rad, or 20.1°. At this fracture angle, the shear stress is calculated as

$$\tau = 35.2 \cos(0.350)/[1.702 * 0.29 \sin(0.850)/\sin(0.350 + 0.850)] = 88.4 \text{ ksi.}$$

The shear stress based on an assumed 45° throat, the normal design asumption, would be $P/(0.707*Ld)$, where d is the smaller of the leg sizes h and v. For the example under consideration, $\tau = 35.2/(0.707 * 1.702 * 0.29) = 101$ ksi, 14% higher than τ calculated using Equation 2.1. The shear stress based on an assumed throat equal to the leg size would be P/Ld, where d is the smaller of the leg sizes h and v. For the example under consideration, $\tau = 35.2/1.702 * 0.29 = 71.3$ ksi, 19% lower than τ calculated using Equation 2.1.

Rockwell B hardness tests of the welds provided an estimate of the weld metal strength. Two welds were tested from each plate, with three points tested per weld, for a total of six readings per plate. Hardness correlates with strength; the correspondences can be found in ASTM A370, Table 2B.

An AWS test plate was welded at each of the two heat inputs for the weathering consumables. All-weld-metal tension specimens were made from these test plates as per AWS D1.65-96 Figures 5.1 and 5.9 and tested in accordance with ASTM A370.

2.3. Results & Analysis

2.3.1. Weathering consumables

Most of the specimens welded one side at a time at high heat input yielded in the base metal instead of fracturing in the weld. The capacities of the welds were thus higher than those that could be calculated based on failure load. The stress in the smallest weld—the highest of the stresses in the four welds—was used to represent the weld stress in these specimens at maximum load. However, weld fractures did not always occur in the weld with the smallest effective area. Failed welds were up to 14% larger than the smallest weld in the same specimen.

Table 2.1 summarizes the test results. Standard deviations are given in parentheses. Shear stresses reported are the average of the three plates and were calculated using Equation 2.1. Rockwell B hardness numbers given are the average of the six readings. The dynamic ultimate stress comes from the all-weld-metal tension test. Four hardness readings were taken from the all-weld-metal section.

Table 2.1. Strength, weathering consumables

Welding method	**measure of strength**	**high heat input**	**low heat input**
Single-sided fillet	**calculated shear stress at failure (ksi)**	77.8 (4.9)	101.6 (9.9)
	Rockwell B hardness	94.8 (0.7)	96.5 (0.6)
Dart-welded fillet	**calculated shear stress at failure (ksi)**	77.3 (3.1)	88.5 (6.3)
	Rockwell B hardness	93.4 (0.6)	92.8 (0.3)
Groove weld (AWS test plate)	**Dynamic ultimate tensile stress (ksi)**	75.5	76.5
	Rockwell B hardness	83.1 (2.8)	82.3 (0.3)

The dynamic ultimate tensile yield stress from the groove weld is close to the fillet weld shear strength for high heat input, but much lower for low heat input. The estimated tensile strengths corresponding to the hardness numbers (from ASTM A370, Table 2B) are 80.1 ksi for the high heat input and 77.9 ksi for the low heat input. The estimated strengths correspond to the measured tensile strengths.

Shear stress is generally estimated at 60% of tensile stress, so the difference between the groove weld tension test and the fillet weld shear test results must be due to different properties of the two welds. Further evidence can be seen in the hardness results. The groove weld hardness is much lower than the fillet weld hardness. The hardness numbers for the shear specimens in Table 2.1 correspond to estimated tensile strengths ranging from 94 to 103 ksi. The shear strength results are still higher than expected for metal with this tensile strength, but there is not as big a discrepancy as that found between the shear strength and the groove weld tensile strength.

Figures 2.11 and 2.12 are graphical representations of the average shear strengths (shear stress at failure) and hardness values, respectively, reported in Table 2.1.

Figure 2.11 shows that the single-sided low-heat welds have the highest average shear strength. There is also apparently a tendency for low-heat welds to have a higher strength than heat-heat welds. From the ANOVA results, the effect of heat input is significant ($p < 0.01$)—low-heat welds are stronger. The effect of welding method is not significant ($p = 0.08$; p below 0.05 is not statistically significant at a 95% confidence level). This can be seen from Figure 2.11: within the high-heat welds, there is no difference at all. The figure does suggest that there might be a significant effect from welding method within the low-heat welds. However, the variability in the data, which is represented by the standard deviations reported in the data table, and which reduces the significance of any differences, is not reflected in the graph. Even within the low-heat welds alone, the difference from welding method is not statistically significant ($p = 0.13$, based on single-factor ANOVA).

On the other hand, the low-heat single-sided welds include the specimens that had base metal failures before the welds reached their ultimate strength. This means that the weld strengths for this group of specimens is actually higher than that recorded, and so the difference might have been significant if the actual strengths had been available.

The effect of welding method on hardness is significant ($p < 0.01$)—single-sided welds are harder. The effect of heat input is significant within single-sided welds ($p < 0.01$, based on single-factor ANOVA)—low-heat welds are harder. The heat input effect is not significant within dart welds ($p = 0.08$).

Overall, low-heat welds are stronger and harder than high-heat welds and single-sided welds are stronger and harder than dart welds. As expected, dart welding and higher heat input have similar effects.

2.3.2. Non-weathering consumables

All specimens failed in a weld. In most cases, the specimen broke in the smallest weld, or if not, then in a weld that was within 5% of the size of the smallest weld. This is within the level of uncertainty in the weld measurement. Only one specimen had a fracture occur in a weld that was significantly larger than the smallest weld. Table 2.2 summarizes the test results.

Table 2.2. Shear strength, non-weathering consumables

welding method	measure of strength	high heat input	low heat input
Single-sided	**calculated shear stress at failure (ksi)**	76.9 (4.0)	88.3 (4.4)
	Rockwell B hardness	91.9 (0.9)	94.8 (1.1)
Dart-welded	**calculated shear stress at failure (ksi)**	76.3 (3.1)	95.6 (7.3)
	Rockwell B hardness	88.4 (1.3)	88.5 (1.3)

The hardness numbers in Table 2.2 correspond to estimated tensile strengths ranging from 87 to 100 ksi. Figures 2.13 and 2.14 are graphical representations of the average shear strengths (shear stress at failure) and hardness values, respectively, reported in Table 2.2.

Figure 2.13 shows that low-heat welds have higher average shear strength. There is does not appear to be much of an effect from welding method. From the ANOVA results, the effect of heat input is significant ($p < 0.01$)—low-heat welds are stronger. The effect of welding method is not significant ($p = 0.27$).

Figure 2.14 shows that the single-sided low-heat welds have the highest average hardness. The effect of welding method is significant ($p < 0.01$)—single-sided welds are harder. The effect of heat input is significant within single-sided welds ($p < 0.01$, based on single-factor ANOVA)—low-heat welds are harder. The heat input effect is not significant within dart welds ($p = 0.93$). Overall, as with the weathering specimens, low-heat welds are stronger and harder than high-heat welds and single-sided welds are stronger and harder than dart welds. As expected, dart welding and higher heat input have similar effects.

2.3.3. Active flux

All of the specimens failed by yielding in the plates rather than fracturing in a weld. Therefore there is no failure strength data available for the welds from this test. The calculated peak shear stresses in the low heat input welds ranged from 55 to 91 ksi, with an average of 80 ksi, and the shear stresses in the high heat input welds ranged from 55 to 83 ksi, with an average of 64 ksi. The lower average stress in the high-heat welds is because the welds had much deeper penetration. The average penetration was 0.13 in for the high-heat welds and 0.05 for the low-heat welds. For both high and low heat inputs, the deepest penetration was 0.18 in, which is much higher than the penetration in any of the welds made with the weathering and non-weathering consumables.

Table 2.3 summarizes the Rockwell B hardness results.

Table 2.3. Rockwell B hardness, active flux

Welding method	high heat input	low heat input
Single-sided	90.2 (3.3)	96.2 (0.5)
Dart-welded	93.4 (1.5)	93.2 (1.1)

The hardness numbers in Table 2.3 correspond to estimated tensile strengths ranging from 89 to 102 ksi. Figure 2.15 is a graphical representation of the average hardnesses reported in Table 2.3. Single-sided low-heat welds have the highest hardness.

The effect of heat input is significant within single-sided welds ($p < 0.01$, based on single-factor ANOVA)—low-heat welds are harder. The heat input effect is not significant within dart welds ($p = 0.86$). The effect of welding method is significant within low-heat welds ($p < 0.01$)—single-sided welds are harder. The heat input effect is not significant within high-heat welds ($p = 0.06$).

The overall pattern is similar to that found for the other two sets of consumables.

2.3.4. Summary

In general, for all consumables, low-heat welds are stronger and harder than high-heat welds and single-sided welds are stronger and harder than dart welds. Both the calculated shear strength and the tensile strength corresponding to the hardness are well above the nominal tensile strength of 70 ksi for all specimens tested.

For all three sets of consumables, no effect of heat input was found within the dart-welded specimens. This may have to do with the effect of dart welding on actual heat input. It is possible that although raising the heat input reduces weld quality, once a “saturation” heat input is reached there will be no more effect from

further heat input increases. If this is so, then dart welding will have no additional effect on a weld whose heat input is already high.

Figures 2.16 and 2.17 summarize the shear strengths and hardness results, respectively, for all consumables. Figure 2.16 reflects the general tendency of high-heat welds to have lower strength. High-heat dart welds have the lowest strength and low-heat single-sided welds have the highest or near-highest strength. Figure 2.17 shows that low-heat single-sided welds also have the highest hardness. The lack of heat effect on hardness in the dart welds can also be seen clearly; the “dart, low” and “dart, high” results are the same for all three sets of consumables.

Shear strength and hardness are plotted against each other in Figure 2.18. Although hardness and shear strength were both subject to the same effects from heat input and welding method, there is no good correlation between the calculated shear stress at failure and the Rockwell B hardness values, for either set of consumables or for the data as a whole. The relationship between hardness and tensile strength has long been established, so the lack of correlation between hardness and shear strength must be due to some aspect of the shear stress determination. Sources of uncertainty for the shear stress calculation include the difficulty in finding the weld area, and the effect that different weld profiles may have on weld performance even for welds of the same total area.

CHAPTER 3: T-BEND TEST

3.1. Fabrication

The specimens were designed based on California Department of Transportation (CALTRANS) specifications, with some modifications to the notch details as described below. Figure 3.1 shows the specimens as provided by the fabricators. Figure 3.2 shows plate dimensions for the welded specimens. The web and flange plates were tacked in place and then welded. The variables were heat input, welding method, and web thickness. 3/8 in and1/2 in web thicknesses were used (only 3/8 in for the non-weathering specimens). The thinner web thickness is intended to simulate a smaller stiffener. The thinner the web, the more likely that dart welding will have an effect on the weld properties. With a thick enough web, the opposing arcs will be far enough away that dart welding will have no effect.

All flange plates were 3/4 in thick. Test specimens were saw-cut from these plates in 2-in slices (Figure 3.3). Table 3.1 gives the current, voltage, travel speed, and heat input used.

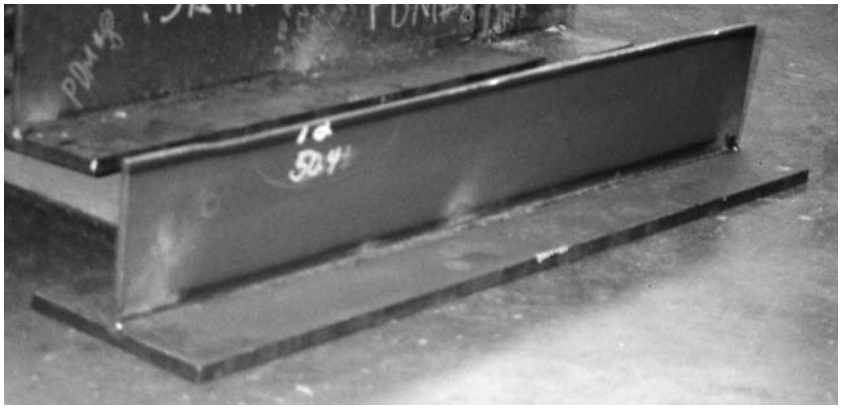

Figure 3.1. T specimens as fabricated

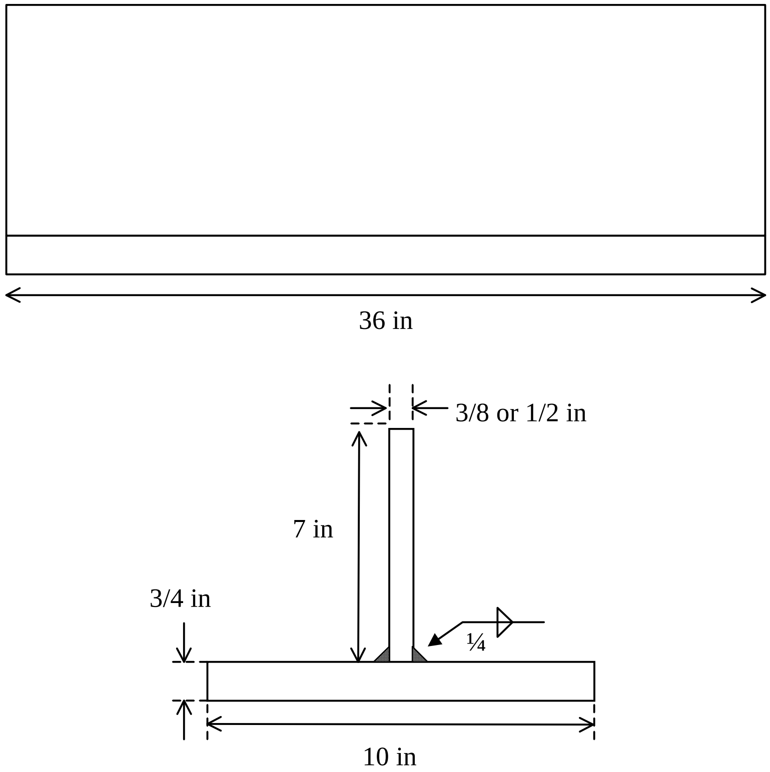
36 in
3/8 or 1/2 in
7 in
3/4 in
¼
10 in

Figure 3.2. T plate dimensions

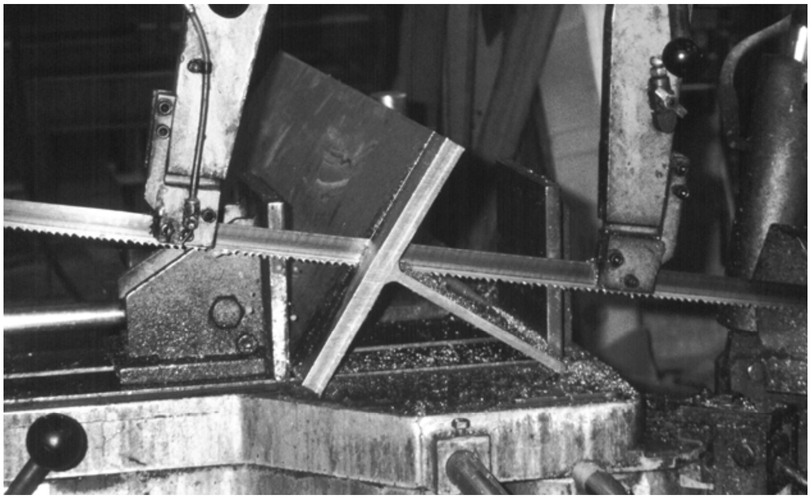

Figure 3.3. Saw-cutting T specimens

Table 3.1. Welding procedure variables

Specimen type	Current (A)	Voltage (V)	Travel speed (in/min)	Heat input (kJ/in)
Weathering, low heat input	300	25	13	34.6
Weathering, high heat input	400	30	15	48.5
Non-weathering, low heat input	310	23	12	35.6
	320	24	14	34.2
Non-weathering, high heat input	360	28	12	50.4
	400	28	14	48.0
Active flux, low heat input	345	23	14	34.0
Active flux, high heat input	430	34	18	48.7

A 60° double-angle cutter with the tip ground to a 5/32-in radius was used to create the notch. Figure 3.4 shows a specimen in the notching setup. Figure 3.5 shows a completed specimen. Figure 3.6 shows the location of the notch on a schematic drawing. The depth of the notch was different for the two web thicknesses, as per the CALTRANS specifications. Those specifications also called for a smaller notch tip radius (1/8 in) for the thinner web (the specified radius was one quarter the web thickness plus 1/32 in), but that would have required two separate cutters, so the larger of the two radii was used for all specimens.

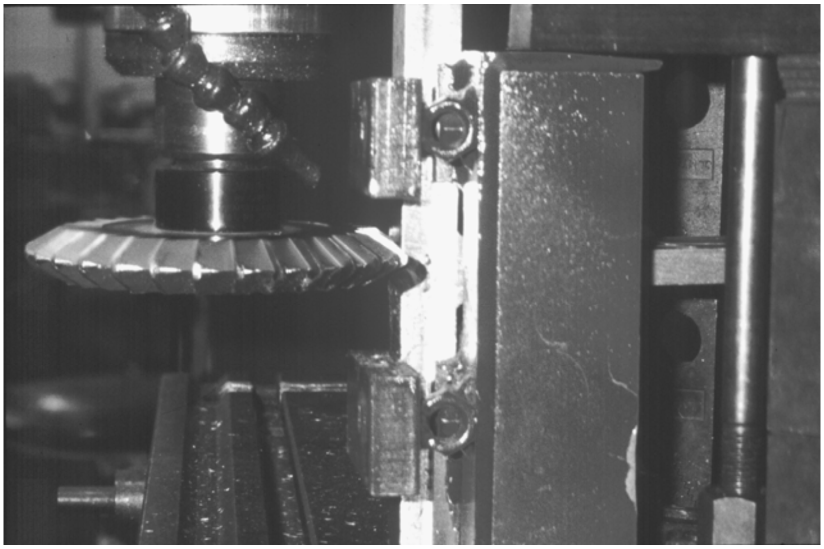

Figure 3.4. T-bend specimen and cutter

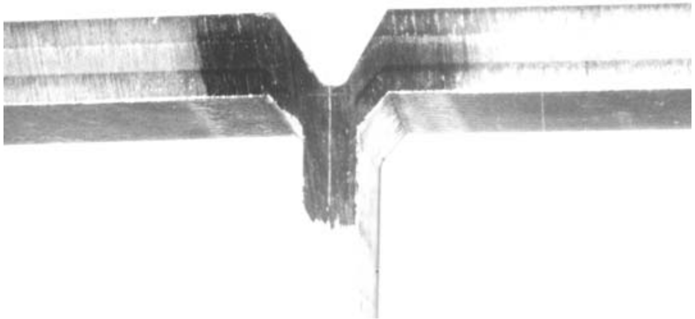

Figure 3.5. Finished T specimen

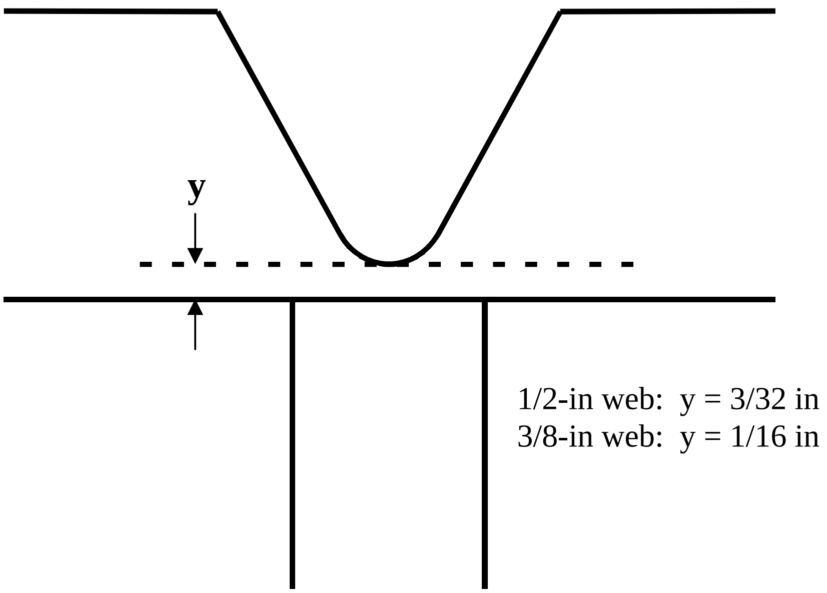

Figure 3.6. Location of notch in T-bend specimen

In some cases the T was not cut exactly perpendicular to the welds, so the notch was skewed with respect to the longitudinal axis of the welds. This was noted in case it had some effect on test results, but no such effect was observed.

3.2. Testing

Figure 3.7 shows a schematic drawing of the test setup. Figure 3.8 shows a specimen in the test fixture, which was bolted to the upper (stationary) head of the testing machine. The web of the T passed through an opening in the upper head. Tension was applied to the web through a bar that was bolted to the end of the web and gripped in the lower (moving) head. Figure 3.9 shows this bar with an earlier specimen that had a 15-inch-long web; later specimens had 7-in webs and the bolt was -hidden by the machine head. The bar was bolted to the T first and then the assembly was dropped through the opening in the head.

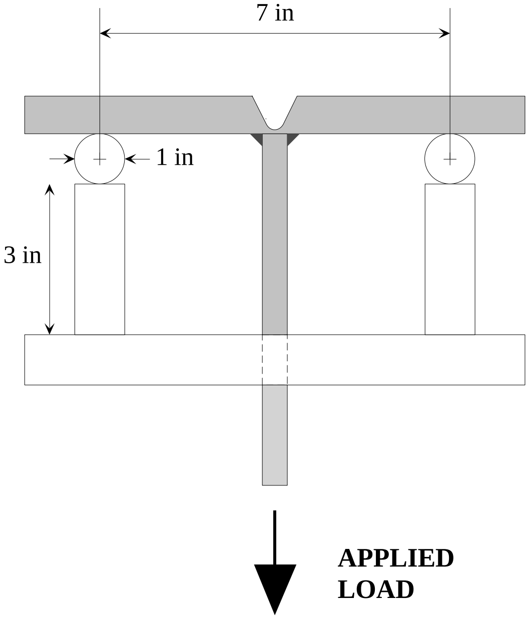
7 in
1 in
3 in
APPLIED
LOAD

Figure 3.7. T-bend test setup

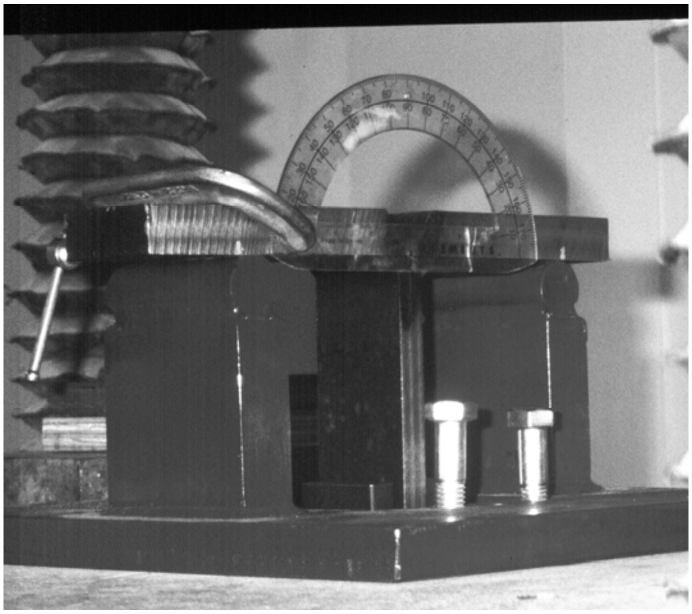

Figure 3.8. T in test fixture

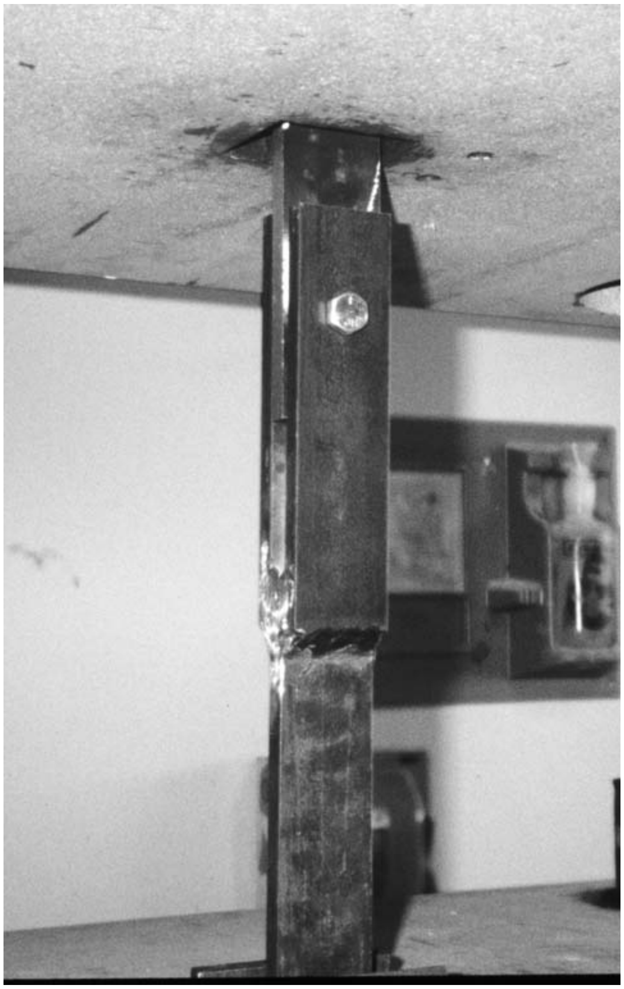

Figure 3.9. Pull bar

The total displacement angle (the sum of the displacements of both arms) was read from a protractor clamped to one arm of the T and the load was read from the machine's dial indicator. Loading was displacement-controlled (loading rate approximately 0.007 in/min) and continued until the notch closed at a displacement angle of about 70° or until the load dropped significantly or rapidly. Some initial tests were stopped when the displacement angle reached 60°. Once the paint wore off the fixture, friction became a problem and an anti-seize compound was applied to the fixture supports. Figure 3.10 shows a specimen during a test, and Figure 3.11 shows a specimen after testing.

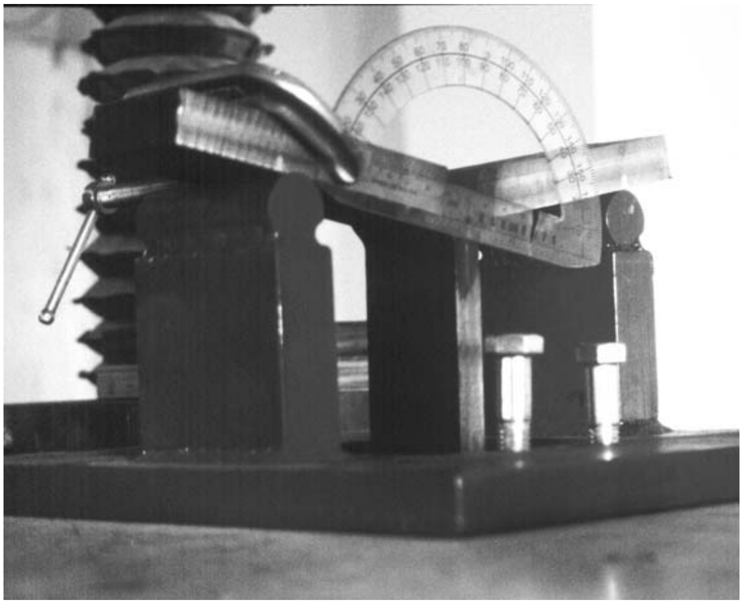

Figure 3.10. T-bend specimen being tested

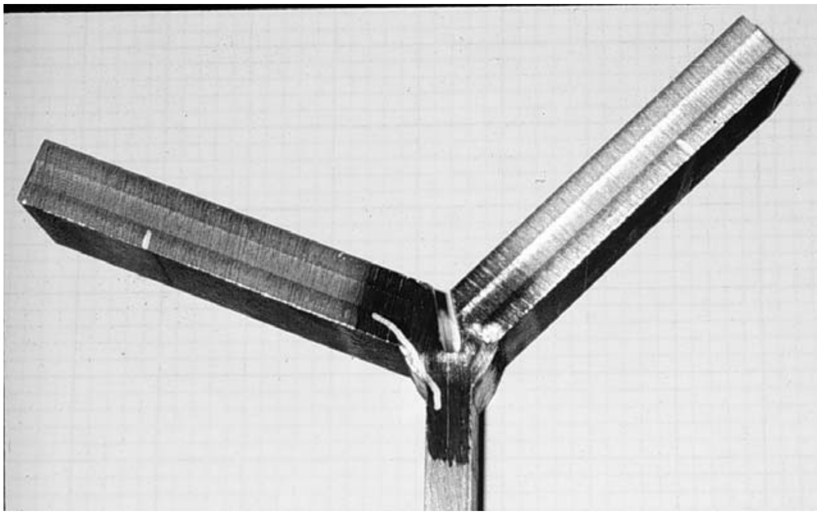

Figure 3.11: T specimen after testing

The fixture supports obstructed the view of the welds. Cracks were usually not visible until after the specimen was removed from the fixture and could be inspected closely. Also, the columns and screws of the testing machine obstructed the face-on view of the specimen; a different design for the pull bar at the bottom would have allowed the specimen to be turned 90° for easier viewing of the displacement angle.

3.3. Results and Analysis

Examples of load-displacement curves are shown in Figures 3.12 to 3.14. The specimen of Figure 3.12 clearly failed at 55°, but there is no such well-defined failure angle in Figure 3.13, and there is no decrease in capacity at all in Figure 3.14. Failure therefore could not consistently be determined from a feature of the curve. The failure angle, shown by circled points in the figures, was defined as the angle at which load dropped to 90% of the peak load, or the angle at which the test was discontinued if there was no such drop. The defined failure angle is 56.5° in Figures 3.12 and 3.13 and falls at the 90%-of-capacity point. In Figure 3.14, the load never dropped to below 90% of the peak capacity before the end of the test, so failure is defined at the end of the curve, at 69.5°. Some of the measured “failure” angles, therefore, are not true measures of the weld flexural capacity. For the first few specimens tested, the test was stopped when the angle reached 60° rather than when the notch closed. For the rest of the specimens, in some cases the notch closed before failure, and in some cases the test had to be stopped because of problems with the test setup—in particular, the protractor sometimes hit the fixture supports at larger angles.

3.3.1. Weathering consumables

3.3.1.1. Visual inspection

Figures 3.15 and 3.16 show examples of welds with a face crack and a toe crack, respectively.

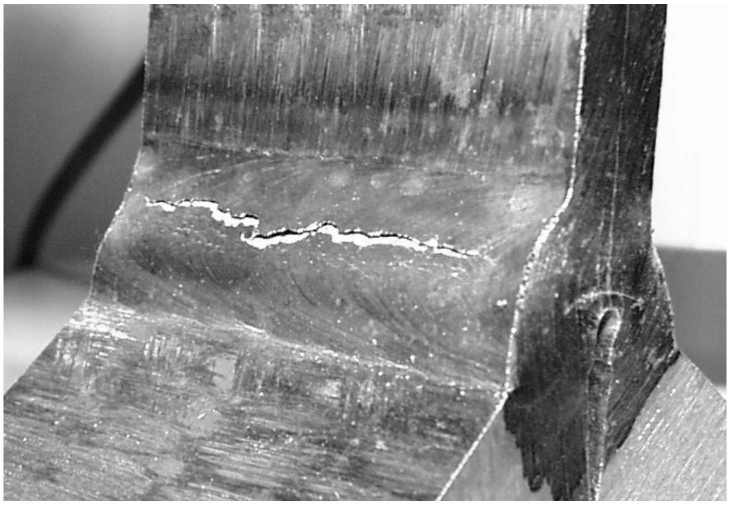

Figure 3.15. Face crack

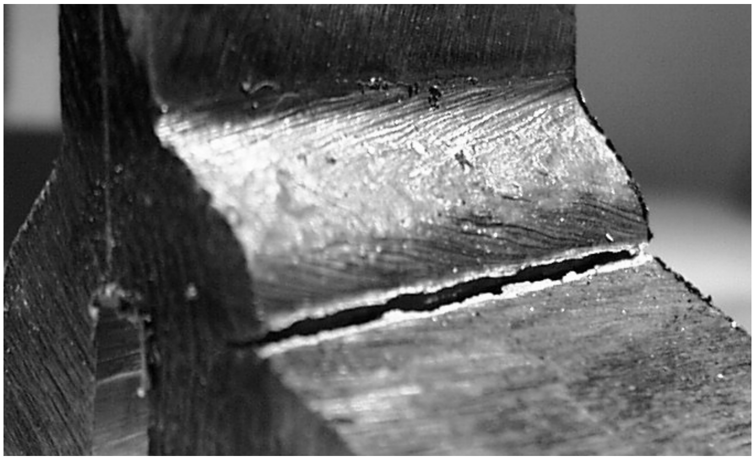

Figure 3.16. Toe crack

There was some grouping in the type of cracking exhibited in the specimens after testing. Of the single-sided specimens, nine had face cracks, one had a toe crack, and two had no obvious cracking at the end of the test. Of the dart-welded specimens, only one had a face crack, four had toe cracks, and eight were not obviously cracked at the end of the test. The high-heat and low-heat groups each had five specimens with face cracks, but the high-heat group had four specimens with toe cracks and four with no obvious cracks, and the low-heat group had only one specimen with a toe crack and six with no obvious cracks. Some specimens had cracks in more than one location. Macroetch inspection revealed that the heat-affected zones of the two welds overlapped in the high-heat dart-welded specimens.

3.3.1.2. Weld capacity

The shape of the load-displacement curve was affected by some of the variables tested. All of the specimens that had no drop in load capacity before the end of the test were dart-welded, and only one of the dart-welded specimens showed the sharp dropoff in capacity typified in Figure 3.12. Most of the low heat input specimens also had only a gradual reduction, if any, in load capacity.

The peak load depended more on the net section remaining after machining than on weld properties. The most obvious indication of this was that the peak loads recorded for the two different web thicknesses occupied entirely separate ranges—under 4000 lb for the 3/8-in web, and over 4500 lb for the 1/2-in web. A true stress calculation would be difficult because of the specimen geometry, and would in any event not be a measure of stress in the weld alone. No such calculation was attempted. The loads were, however, normalized with respect to the width of the specimens, which was the weld length. The angle change measured was the total change for both arms, so the normalized load was defined as the total load supported divided by the total weld length for both sides.

No statistically significant relationship was found between peak load and either method or heat input, even when the results for each web size were considered separately.

Failure angles are plotted against peak loads in Figure 3.17. The separation of the results for the two web sizes is clearly seen, and within each of the web sizes there is quite a bit of scatter. There is no statistical correlation between the angles and the loads. There are no strong patterns in the distribution of either welding method or heat input.

3.3.1.3. Hardness

Table 3.2 summarizes the Rockwell B hardness results. Standard deviations are given in parentheses. The hardnesses correspond to tensile strengths ranging from 92 to 105 ksi.

Table 3.2. Rockwell B hardness, weathering T specimens

welding method	high heat input	low heat input
1/2-inch web		
single-sided	96.4 (2.5)	97.2 (1.7)
dart-welded	92.3 (2.0)	95.9 (1.3)
3/8-inch web		
single-sided	96.4 (1.7)	95.1 (2.5)
dart-welded	92.3 (1.7)	91.9 (3.6)

Bar graphs of the hardness results are presented in Figures 3.18 to 3.20. Figure 3.18 primarily shows the effect of welding method, Figure 3.19 web thickness, and Figure 3.20 heat input. The effect of welding method was significant overall ($p < 0.01$ based on three-way ANOVA)—single-sided welds were harder than dart welds. The effect of web thickness was significant only among the low-heat welds ($p < 0.01$ based on two-way ANOVA within low-heat data)—the specimens with 1/2-inch had harder welds than the specimens with

3/8-inch webs. Heat input had a significant effect only among the specimens with 1/2-inch webs ($p < 0.01$).

As was seen in the shear test, the lower-heat and single-sided welds are harder. In addition, the specimens with 1/2-inch webs are harder as well. There should be a web size effect among the dart-welded specimens because a thicker web provides a greater distance between opposing arcs and so the heat input will not increase as much. This effect was seen only among the low-heat dart welds and not the high-heat dart welds. This might be explained by the "saturation" concept suggested at the end of Chapter 2, that a weld already weakened by one adverse condition will not be further weakened by another. However, web size also had an effect on the low-heat single-sided welds. The only effect the smaller web size should have on single-sided welds is a relatively larger penetration into the plate. The problem with thin webs that was reported by Miller (1997) and described in Chapter 1 only occurs when welds are made on both sides simultaneously.

3.3.2. Non-weathering consumables

Only 3/8-inch webs were used. Within each heat input category (high and low) there were two sets—one with higher current and travel speed, and one with lower current and travel speed (refer back to Table 3.1). The higher heat input within each category (with slower travel speed) corresponded to the procedure used in other tests (tensile and Charpy V-Notch) on the same set of consumables. Failure angles are plotted against heat input in Figure 3.21. The differences in heat input do not seem to have much of an overall effect on the ductility. Normalized peak loads are plotted against heat input in Figure 3.22. Within each heat category, the specimens made with the slower travel speed, at the slightly higher heat input, tend to higher peak loads. Both of the dart-welded high-heat

specimens were cracked in places at fabrication. Test slices were cut from uncracked sections of the specimens.

One of the specimens (single-sided, 50.4 kJ/in) showed aberrant load-displacement behavior and was not considered for analysis. Its load-displacement curve is shown in Figure 3.23. Instead of reaching a peak somewhere around 3000 lb, the load continued to increase until the test was stopped when the end of the machine's scale was reached at 6000 lb. At this point the load was still increasing sharply. Another specimen cut from an adjacent location in the plate behaved normally, with a curve resembling that in Figure 3.13.

3.3.2.1. Visual inspection

All but three of the specimens had cracks at the weld face after testing. Only two specimens cracked at the weld toe; both were low heat input. This was not the pattern seen with the weathering consumables, in which most of the specimens that cracked at the toe were welded with a high heat input. With only two such cracks, though, perhaps conclusions should not be drawn. There were two specimens that had little or no cracking at the end of the test; both were dart-welded.

The heat-affected zones overlapped in all the dart-welded specimens and in the very highest heat input (50.4 kJ/in) of the single-sided specimens.

3.3.2.2. Weld capacity

The patterns of load-displacement behavior were not as well defined as for the weathering materials. Five of the seven specimens that had a sudden drop in capacity were welded one side at a time, which is a similar effect to that found among the weathering specimens. Another five of those seven specimens were also welded at the higher travel speed.

Failure angles are plotted against peak loads in Figure 3.24. The dart-welded specimens undergo the largest distortions while carrying the highest

loads. The effect of welding method on load carried should not simply be a matter of weld cross-section; the outer profile of the weld should be the same for dart welds and single-sided welds because the equipment used to make them is the same and used at the same orientation. The only trend in weld profile seen in these specimens is that the weld profiles of the single-sided 3/8-inch specimens are slightly flatter (forming a larger angle with respect to the web) than the profiles of the dart-welded specimens. Penetration should not be a factor in this test because the gap closes in compression, and fractures start at the outer surfaces of the welds.

The high-heat specimens carry the highest loads, but there does not seem to be any effect of heat input on ductility; the two heat input categories have roughly the same range of displacement angles. The high-heat, dart-welded specimens had the best performance in this test in terms of load capacity and ductility, even though these were the specimens that cracked during fabrication. This shows that the T-bend test does not predict that a particular welding procedure may produce a weld that is prone to cracking.

3.3.2.3. Hardness

Table 3.3 summarizes the Rockwell B hardness results. Standard deviations are given in parentheses. The hardnesses correspond to tensile strengths ranging from 82 to 102 ksi.

Table 3.3. Rockwell B hardness and estimated tensile strength (ksi), non-weathering T specimens

welding method	high heat input	low heat input
slow travel speed		
single-sided	92.7 (0.8)	92.6 (1.7)
dart-welded	89.2 (1.1)	91.8 (0.9)
fast travel speed		
single-sided	93.4 (1.4)	96.1 (2.5)
dart-welded	85.4 (2.8)	88.9 (2.0)
overall (both travel speeds combined)		
single-sided	93.0 (1.2)	94.3 (2.7)
dart-welded	87.3 (2.9)	90.4 (2.1)

There was no consistent effect of travel speed on hardness. The two travel speeds were combined and a two-factor ANOVA was performed. The effects of both heat input and welding method were statistically significant ($p < 0.01$). As with other specimens and other tests, low-heat and single-sided specimens had harder welds. Figure 3.25 is a graphical representation of the hardness results for both travel speeds combined. Both the heat effect and the method effect can be seen. The low-heat single-sided specimens had the highest hardness and the high-heat dart-welded specimens had the lowest hardness.

3.3.3. Active flux

With the higher heat inputs, the fabricator had trouble maintaining the weld at the 1/4-inch size required. To keep the size down, the travel speed had to be increased, and the current had to be raised to compensate. The fabricator stated that these welds would not be optimal. The low heat input welds were welded using the fabricator’s usual procedure.

3.3.3.1. Visual inspection

In all of the specimens welded at a high heat input, for both web thicknesses, there was complete fusion across the web, as shown in Figure 3.26. Among the specimens welded at the lower heat input, the dart-welded specimens had overlapping heat-affected zones. Most of the high-heat specimens failed at smaller angles than the low-heat specimens, with the exception of the single-sided thin-web group, in which there was not much separation of failure angle by heat input.

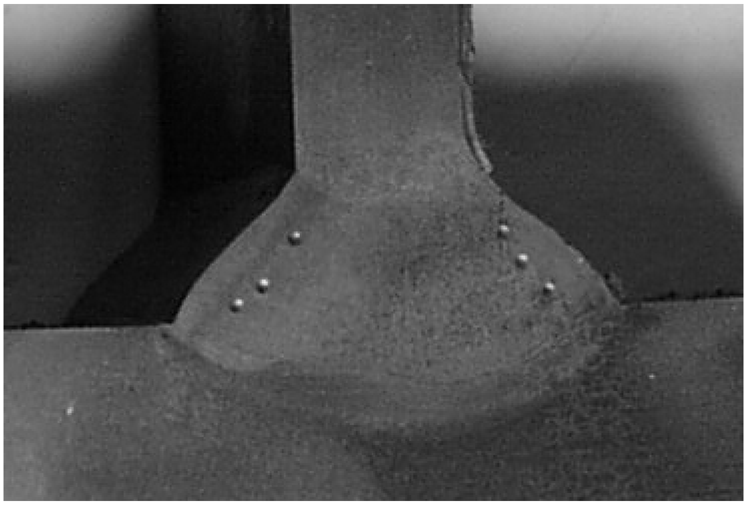

Figure 3.26. Complete fusion across 3/8-inch web

One set, the high-heat dart-welded specimens with 3/8-inch webs, exhibited fractures similar to the kind described by Miller (1997). An example is shown in Figure 3.27. Although these specimens did not appear to be cracked on the surface, cracks through the weld developed very quickly during the tests, in exactly the location described by Miller. A close inspection of the fracture surface revealed dark areas, indicating prior cracking.

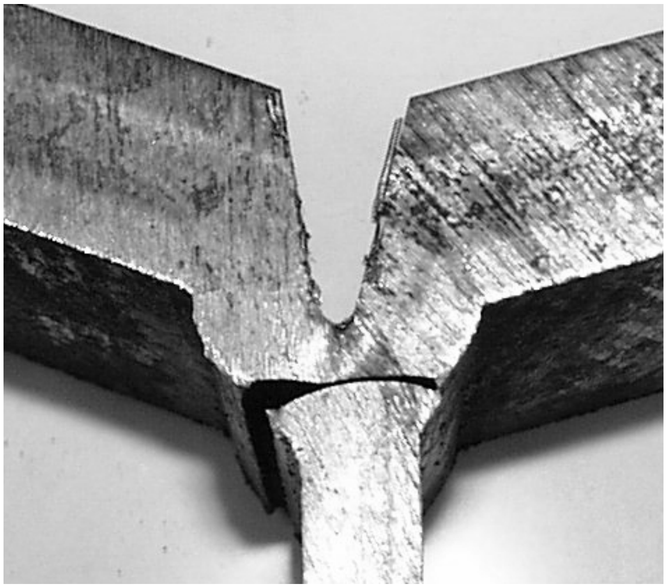

Figure 3.27. Crack in high-heat dart-welded T

These specimens were welded under the circumstances most likely to produce such cracks. The already high heat input is augmented by dart welding across a thin web. Miller states that this effect occurs only with webs thinner than 3/8 in. However, the heat input to the weld in the active flux specimens was, in the opinion of the fabricator, excessively high for the type of weld desired; this extraordinarily high heat input may have been enough to cause melt-through even with a web normally thick enough to prevent this.

Eight of the low-heat specimens had face cracks, three had toe cracks, and one was not obviously cracked at the end of the test. Nine of the high heat specimens had toe cracks, three had the type of fracture seen in Figure 3.27, one had a face crack, and one was not obviously cracked at the end of the test. Some specimens were cracked in more than one location.

3.3.3.2. Weld capacity

Most of the specimens that had a sudden drop in strength early in the test had been welded at the higher heat input, which may confirm the fabricator's assessment that these welds would not perform well. The low-heat specimens with this failure mode were dart-welded with a 3/8-inch web; these circumstances lead to an increased total heat input to the welded area, so performance similar to that seen in high-heat welds is expected.

Failure angles are plotted against peak loads in Figure 3.28. For the effect of heat input, only the thick-webbed specimens show a clear pattern. Among these, the high heat input specimens all failed at much smaller angles than the low heat input specimens, which is consistent with results for the other consumables within this test and with the shear test results. The single-sided high-heat specimens showed particularly poor ductility.

In the case of the thin-webbed specimens, the low-heat specimens fall between the dart-welded and single-sided groups within the high-heat specimens for both peak load and failure angle, with the dart-welded high-heat specimens failing at very small angles and low loads. These particular specimens will be further discussed below. Only the dart-welded specimens that broke in the manner shown in Figure 3.27. There is no other pattern of fracture type related to welding method.

3.3.3.3. Hardness

Table 3.4 summarizes the Rockwell B hardness results. The hardnesses correspond to tensile strengths ranging from 86 to 106 ksi.

Table 3.4. Rockwell B hardness, active flux T specimens

Welding method	high heat input	low heat input
1/2-inch web		
Single-sided	94.3 (1.2)	96.2 (1.7)
Dart-welded	91.6 (1.5)	92.3 (2.3)
3/8-inch web		
Single-sided	90.3 (1.8)	97.3 (1.5)
Dart-welded	88.2 (3.7)	92.5 (1.3)

Bar graphs of the hardness results are presented in Figures 3.29 to 3.31. Figure 3.29 primarily shows the effect of welding method, Figure 3.30 heat input, and Figure 3.31 web thickness. The effects of both welding method and heat input are significant ($p < 0.01$)—low-heat welds are harder than high-head welds, and single-sided specimens have harder welds than do dart-welded specimens. The effect of web thickness was significant only among the high-heat welds ($p < 0.01$ for high-heat data; $p = 0.38$ for low-heat data)—specimens with 1/2-inch webs have harder welds than specimens with 3/8-inch webs. The lack of web thickness effect among the low-heat welds may be because the lower heat input is not enough to have an effect across an 3/8-inch web and therefore will also not have an effect across a thicker web. The effects of the three variables are the same as those seen for the other consumables and for the shear test where applicable: high heat, dart welding, and thinner web all correlate with lower hardness.

3.3.4. Summary

The non-weathering consumables were the most likely to show face cracks. Almost every specimen showed face cracks at the end of testing. The weathering consumables were the materials least prone to visible cracking, but the most likely to have toe cracks. With these consumables, single-sided welds were

more likely to have face cracks and dart welds were more likely to have toe cracks. The dart welds were also less likely to be cracked at all. High heat input welds made both with the weathering consumables and with the active flux were more likely to show toe cracks than low heat input welds. The active flux low-heat welds were more likely than the high-heat weld to show face cracks. This suggests an overall tendency for high-heat welds to crack at the weld face while low-heat welds crack at the toe. With the weathering consumables, dart welds and high-heat welds share the tendency to have toe cracks. For weathering and non-weathering consumables, dart welds were more ductile than single-sided welds, but high-heat welds were less ductile than low-heat welds.

The active flux performance at high heat input was poor, as predicted by the fabricator. At the lower heat input tested, which is the highest heat input the fabricator would use in production, the active flux was no worse than the non-weathering consumables for cracking, and performed at least as well as the other two sets of consumables in terms of load supported. This weld material performed at least as well as the other two materials in terms of ductility except in the case of the dart-welded thin-web specimens, which failed at smaller angles even with the lower heat input. Apparently high heat input is a serious problem for the active flux combination, and circumstances that increase the heat input, such as dart welding across thinner webs, must be carefully considered. An even lower heat input may be required for these welds, or else the arcs must be staggered rather than directly opposing.

The Rockwell B hardness results for all the specimens are compiled in Figure 3.32. The overall pattern for all consumables is that low-heat welds are harder than high-heat welds, single-sided specimens have harder welds than dart-welded specimens, and specimens with thicker webs have harder welds than

specimens with thinner webs. The tensile strength corresponding to the hardness is well above the nominal strength of 70 ksi for all specimens tested.

CHAPTER 4: WELD ROOT CVN TEST

4.1. Fabrication

A WRCVN plate was made for each of the two heat inputs for each set of consumables. An AWS standard test plate was made for each of the two heat inputs for the weathering consumables.

The AWS standard plate requires a groove weld large enough to include the cross section of an all-weld-metal tensile specimen with 3/4-in diameter threaded ends. The CVN impact blocks are cut so that the V-notch is located at what was the center of the groove weld, which bears no similarity at all to a fillet weld.

Figure 4.1 shows the specification drawing for the plate from which the WRCVN impact blocks were machined. A natural notch is formed between the two plates in the land area below the bevel. The first pass of the 60° groove weld simulates a fillet weld. Figure 4.2 shows the location of the CVN specimen within the plate. Enough passes were made to provide sufficient depth of weld to include the 10-mm specimen. The machined impact blocks as finished were to have a 2-mm natural notch, so the required depth of weld was 8 mm. In most cases this took three or four passes. In the case of the high-heat active flux weld, the first pass penetrated so deeply into the land area that six passes were required. Fabricators were required to minimize bending of the final specimen; excessive bending would not have allowed standard-length CVN specimens to be taken. One fabricator prevented bending by tacking support plates to the work piece and to the table (Figure 4.3); another used clamps.

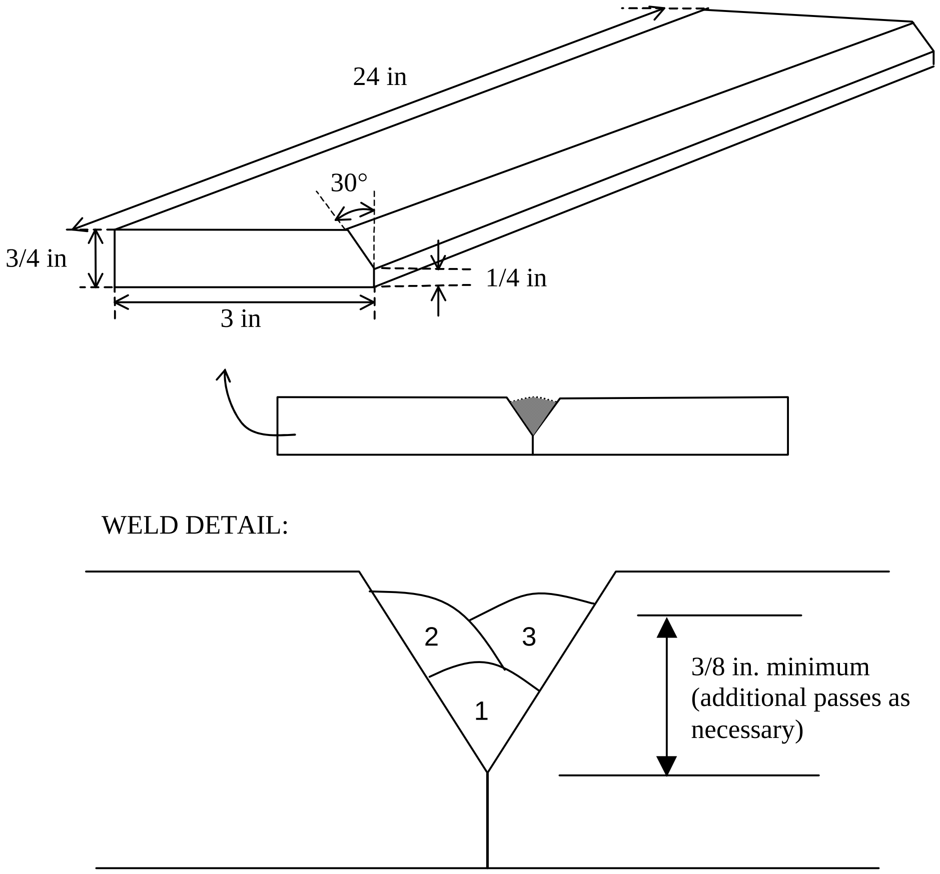
24 in
30°
3/4 in
1/4 in
3 in
WELD DETAIL:
2
3
1
3/8 in. minimum
(additional passes as
necessary)

Figure 4.1: WRCVN plate

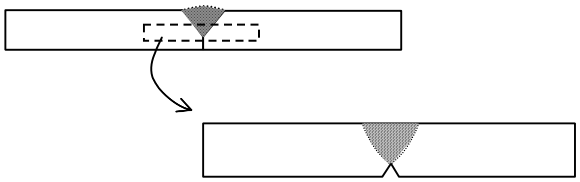

Figure 4.2: Location of CVN impact bar within WRCVN plate

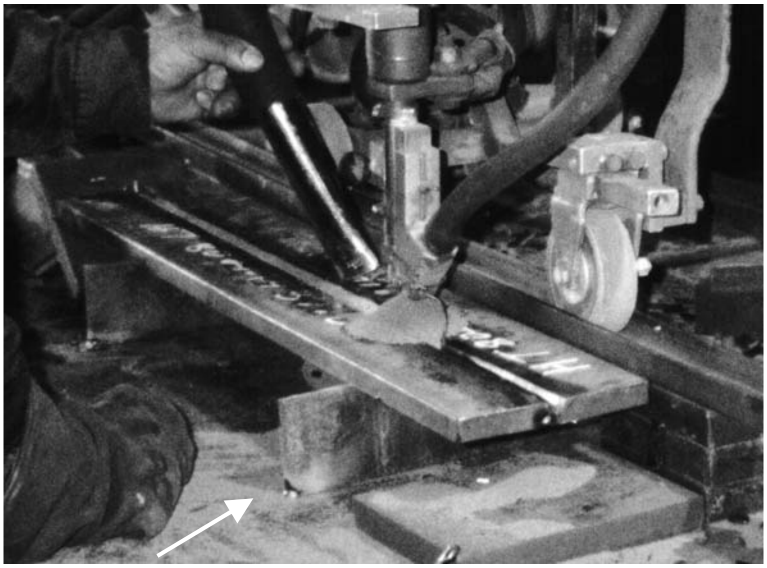

Figure 4.3: Plates used to prevent bending

Placement of the natural notch to align with the machined V-notch required more precise machining than that needed for preparation of ordinary CVN specimens. The procedure was as follows:

1. A section with width slightly greater than the final specimen length was cut from the plate, centered on the weld (Figure 4.4).

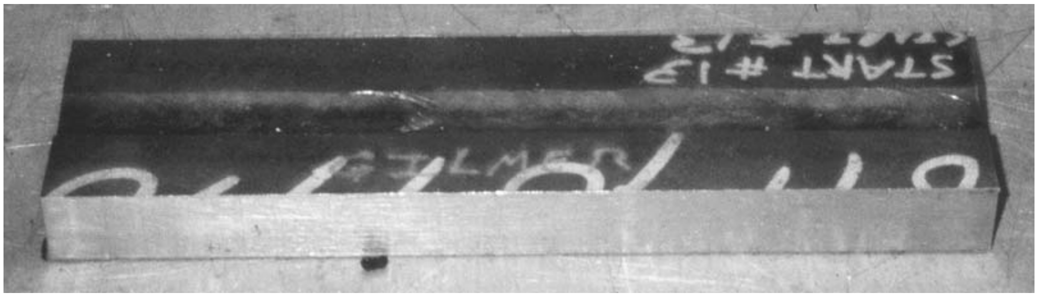

Figure 4.4: Section of WRCVN plate containing weld

2. The top surface (opposite the side with the natural notch) was milled to provide a flat reference surface.

3. The bottom surface was milled to a natural notch depth of 2mm (Figure 4.5), so that the tip of the V-notch would be at the very root of the weld. Shims were used to ensure as even a natural notch depth as possible (Figure 4.6).

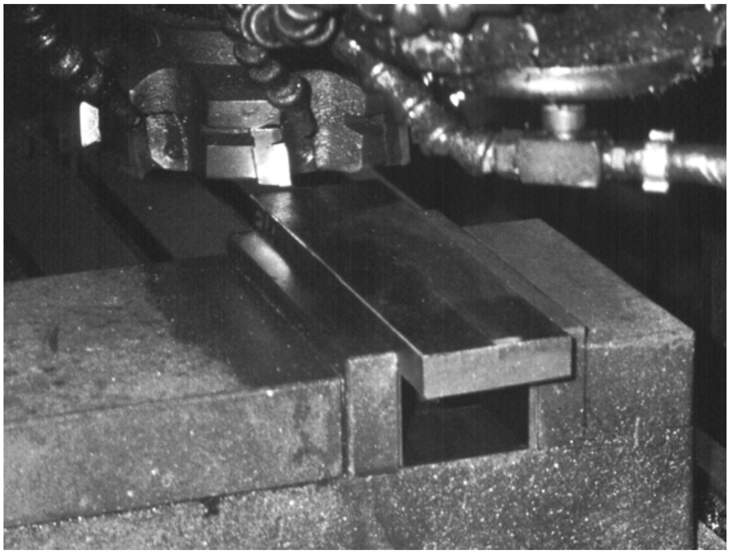

Figure 4.5: Milling the natural notch side of the plate

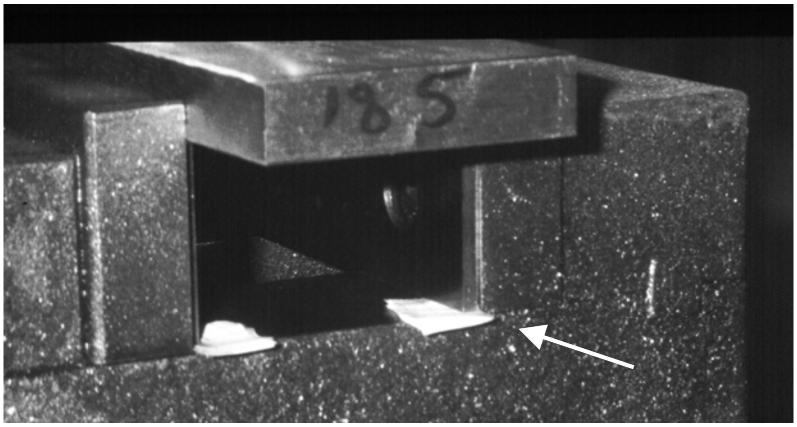

Figure 4.6: Shims used to maintain consistent natural notch depth

4. The blocks were milled to a width equal to the specified length of a CVN specimen, with the natural notch centered along the block (Figure 4.7).

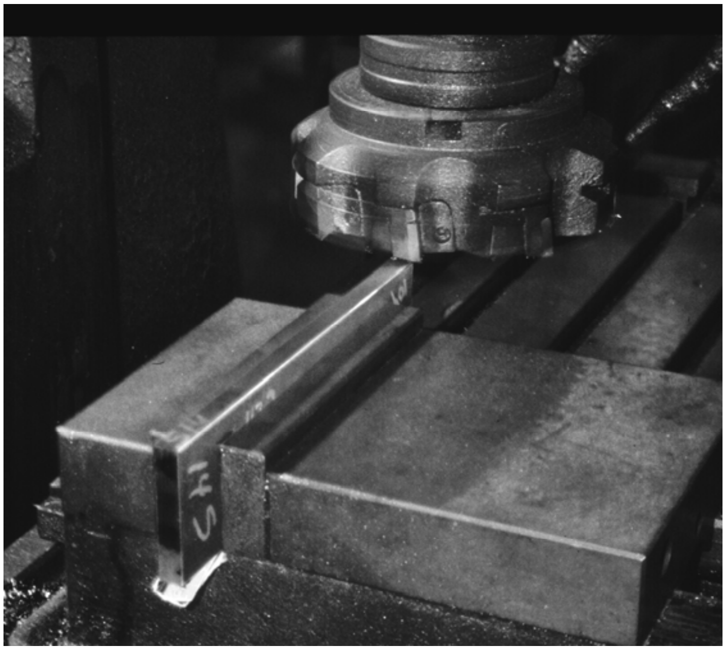

Figure 4.7: Milling edges to appropriate width

5. The blocks were saw-cut into 1/2” pieces and milled to final CVN impact block dimensions.
6. A 45° V-notch was cut as in standard CVN specimens. The V-notch was cut to align as closely as possible with the natural notch. A reference line was scribed around the specimen at the location of the natural notch, and this line was aligned with the center of the V-notching broach.

Some specimens did not meet the CVN specification for centering of the V-notch (notch more than 1/8” off center). This did not appear to affect the manner in which the specimens broke. The specification is intended to ensure that the impact block can break without an end catching in the fixture holding it in place if it is too long or not being held at all if it is too short. The blocks that did not meet the specification showed the same marks from the fixture as did the blocks that did meet the specification.

During testing it was determined that if the V-notch was slightly misaligned with the natural notch, the test results were not affected. However, any specimens accidentally notched on the wrong side were rejected because the cross-section area to be broken was too small—6 mm deep instead of 8 mm.

It is unrealistic to expect to machine the natural notch depth to exactly 2 mm in all specimens because the penetration of the first weld pass varies slightly along the length of the plate. (Hahin's plates were cut into 1/2-in strips first and these strips machined individually, so the natural notch depth was better controlled.) The natural notch must be 2 mm deep or less. Otherwise, the natural notch will be deeper than the V-notch, and the cross section to be broken will be less than the specified requirement of 8 mm. Some specimens were discovered after testing to have had the natural notch extending beyond the V-notch. These test results were disregarded and new specimens tested, because the specimens with the deep natural notch should have been rejected before testing.

Figures 4.8a and 4.8b show the location of the weld within the specimen, revealed with acid etching, and the location of the machined V-notch with respect to the natural notch and the weld. The different weld passes and heat-affected zones can been seen in these figures as well. Standard test plates (AWS D1.5-96 Test Plate A) were made at both heat inputs using the weathering consumables.

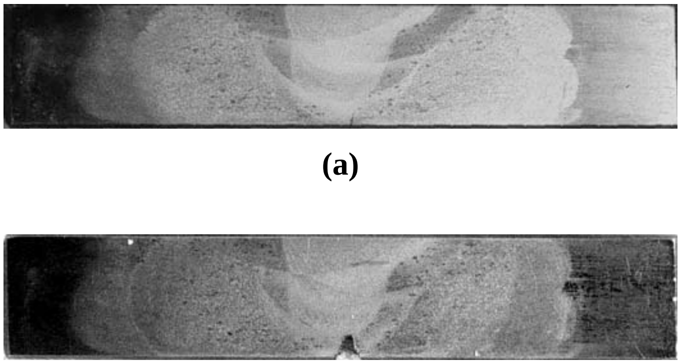

(a)

(b)

Figure 4.8. WRCVN specimen (a) before and (b) after notching

4.2. Testing

Testing was done as per ASTM A370 at 20° C intervals from -40° C to +60° C for the non-weathering and active flux specimens and from -20° C to +60° C for the weathering specimens. Additional active flux specimens were tested at –30° C. Two specimens were broken at each temperature from each plate. In addition, the natural notch depths were measured prior to testing for some of the weathering specimens, which were then V-notched and broken at 0° C. This was done to determine the influence of the depth of the machined notch into the root of the weld.

4.3. Results and Analysis

4.3.1. Effects of heat input and consumables

CVN results for the weathering, non-weathering, and active flux specimens at both heat inputs are plotted in Figures 4.9 to 4.11, respectively. In both the non-weathering (Figure 4.9) and weathering (Figure 4.10) WRCVN specimens, the higher heat input welds had a somewhat higher CVN toughness. The effect of heat input is clearer among the weathering specimens (Figure 4.9).

For this combination of consumables, at most temperatures, both high-heat WRCVN specimens had higher CVN toughness than either of the low-heat specimens. There is not as much separation in the results for non-weathering specimens (Figure 4.10).

In Figure 4.9, results are reported for both the WRCVN and the AWS standard specimens. The AWS standard specimens have a much higher CVN toughness than the WRCVN specimens. This indicates that the AWS standard specimens considerably overestimate the toughness of fillet welds and are not good predictors of fillet weld characteristics. In addition, the lower heat input welds had a higher CVN toughness among the AWS standard specimens, while the general trend among the WRCVN specimens for both weathering and non-weathering consumables was for higher-heat welds to have a higher CVN toughness.

There was no clear effect of heat input among the active flux specimens (Figure 4.11). The active flux high-heat specimens may not be expect to behave in the same way as the other specimens because the first pass burned all the way through the land area of the plate, leaving no natural notch. The V-notch was therefore several mm away from the weld root. This was the test plate that required six passes to fill the groove.

Because there was no visible natural notch in the high-heat specimens, an error was made in marking these specimens during machining, and the first set of impact blocks tested was revealed later through acid etching to have been notched on the wrong side, away from the weld root. There were not enough remaining specimens to redo the entire run of tests, but the tests were redone for a few of the temperatures, with the same lack of effect of heat input and high degree of scatter. Apparently, with no natural groove remaining at all, there is nothing resembling a fillet weld root in the specimen, so it does not matter which side the V-notch is on. However, a heat input effect similar to that found in the standard AWS specimens (Figure 4.9) should be expected, and was not found. The results reported in Figure 4.11 are the original run of tests, with the V-notches on the side further from the first weld pass.

Table 4.1 reports the significance levels for the effect of heat input based on a two-way ANOVA within each set of consumables, with temperature and heat input as factors. Only the temperatures common to all sets of specimens were included in the ANOVA: -20° C to 60° C in 20° intervals.

Table 4.1. CVN toughness, ft-lb (average over full temperature range)

Consumables	**low heat input**	**high heat input**	**Significance of difference**
weathering, WRCVN	70.2	79.8	Significant at 99% confidence level ($p < 0.01$)
weathering, AWS standard	114.0	103.7	Significant at 99% confidence level ($p < 0.01$)
non-weathering	59.9	68.2	Significant at 95% confidence level ($p = 0.05$)
active flux	42.1	49.9	Not significant ($p = 0.18$)

As suggested by the plots, the effect of heat input is stronger for the weathering specimens than for the non-weathering specimens, but is significant in both cases, and is not significant for the active flux specimens. Figure 4.11 also shows that the active flux specimens at the very lowest temperatures do not meet the standard of AWS D1.5-96 for temperature zone III, which requires a minimum of 20 ft-lb (27 N-m) at –30° C.

Results for the three sets of consumables used (WRCVN specimens only) are compared in Figures 4.12 and 4.13 for the low and high heat inputs,

respectively. For both high and low heat input, the weathering specimens have the highest CVN toughness and the active flux specimens the lowest, especially at higher temperatures. This cannot be an effect of the slight difference in heat inputs used for the three sets, because the weathering specimens were made using a lower heat input than the non-weathering specimens.

The data point marked "unusual break" was a low-heat non-weathering specimen, numbered P13-19, that broke along the weld interface. Figure 4.14 shows a photograph of the broken specimen. In Figure 4.15 the specimen has been etched and the weld can be seen. The weld is more or less symmetrical, and the shape of the break on one side of the weld matches the shape of the weld on the other side. This specimen was broken at 40° C. The specimens from adjacent locations in the plate were broken at lower temperatures and did not show this effect. Three other specimens from nearby in the plate were later broken at 40° C; the specimen that was cut from the location closest to specimen P13-19, about an inch away, also broke in this manner. The specimens that broke along the weld interface had lower CVN toughness than other specimens tested at the same temperature that broke through the weld.

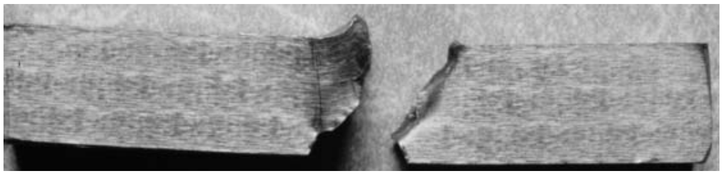

Figure 4.14: Break along weld interface

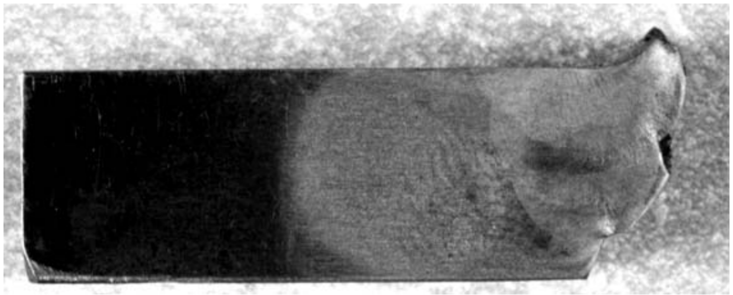

Figure 4.15: Break along weld interface, etched

4.3.2. Effect of depth of V-notch into weld

The shallower the natural notch after milling, the deeper the machined V-notch extends into the weld root. Figure 4.16 shows CVN toughness plotted against natural notch depth after milling. The depth reported is the average of the depth measured on either side of the specimen, and is expressed as a fraction of the specified depth of 2 mm. A lower ratio means that the tip of the machined notch was deeper into the root of the weld. All specimens were broken at 0° C. There is clearly a great deal of scatter in the data. Somewhat of a trend might be seen in the low-heat data—the toughness is higher for shallower natural notches, i.e. for V-notches deeper into the weld. This might be expected because the weld material further away from the root will be closer to the second root pass and may have a more refined crystalline structure. However, if this were a meaningful trend, a similar parallel trend should be found in the high-heat data, and there is none.

CHAPTER 5: SUMMARY AND CONCLUSIONS

5.1. Evaluation of tests

5.1.1. Strength tests

The all-weld-metal tension test does not reflect fillet weld characteristics, so there should be no need for the very large groove weld used in the AWS standard plate. The shear test may or may not reflect the type of stresses that fillet welds are subject to in the field. A longitudinal weld specimen might be more realistic, but much harder to fabricate efficiently. If a transverse weld is used to qualify a procedure that will be used to make a weld subject to longitudinal forces, a higher strength should be required of the test specimen than that required of the production weld. The shear test is not recommended for accurately determining weld strength because of the difficulties involved in determining the weld area.

However, such testing may not be necessary at all. The shear tests show that welds are much stronger than the nominal electrode strength, and also stronger than the design strength that assumes shear fracture on a 45° throat. Tests were run on specimens from three different fabricators using three sets of welding consumables, at two different heat inputs, and with both dart welding and single-sided welding. In all of these cases the weld strength exceeded requirements. This suggests that extensive strength testing by fabricators should not be required, as long as the weld workmanship is appropriate and the electrode manufacturer maintains sufficient product quality. An estimate for weld strength can be obtained from the Rockwell hardness test.

5.1.2. T-bend test

The T test measures weld ductility, not strength. It is difficult to evaluate and use results from this test. The entire run of tests taken as a whole gave some information about the effects of the test parameters, but testing a single T does not tell much about the particular weld used to make that T. However, even if the T-bend test is not of much use, a T specimen is still valuable. The T macroetch specimen, already required by AWS D1.5-96 §5.10.3, can be used for hardness testing of joints welded to the same fillet weld specifications to be used in the field (e.g., same plate thicknesses, use of single or dart welds, number of passes). The macroetch test can also be used to prevent deep fusion from high heat input.

5.1.3. Weld-Root CVN test

WRCVN specimens had different properties from standard AWS CVN specimens. The WRCVN specimens should reflect fillet weld properties more accurately because they are taken from the root of what is in essence a multiple-pass fillet weld. If the pattern seen among the weathering specimens can be extrapolated to other consumables, then the standard test overestimates weld toughness. On the other hand, fillet welds have been made to the current toughness standard for years with no apparent problems in the field, so apparently the actual fillet weld toughness does not need to be as high as that called for the standard.

The WRCVN test does not determine strength, but the Rockwell hardness test, performed either on the WRCVN specimen or, better, a T specimen made with the same welds and welding methods that will be used in production, could be used to ensure adequate strength. Strength is generally not the critical property in fillet weld testing if adequate weld quality is maintained and appropriate materials are chosen.

Another drawback of the WRCVN test is that the effect of dart welding on toughness cannot be tested. A specimen with a thin enough web for dart welding to have an effect will not be large enough to have a CVN specimen taken from it. However, the effect of dart welding is due to the increase in total heat input, and so this effect may be simulated by using a higher heat input. Additionally, the difference due to heat input among specimens of the same type is far smaller than the difference between the WRCVN and the AWS CVN specimens. Even if the effect of dart welding is neglected, the WRCVN test will still give a more accurate representation of the fillet weld CVN toughness than the AWS CVN test does currently.

5.2. Welding consumables

If appropriate precautions are taken regarding heat input, the active flux combination (780/L-61) performs at least as well as the well-established weathering (860/LA 75) and non-weathering (960/L-61) consumable combinations. The CVN toughness of the active flux welds is lower than that of the other weld metals and does not meet current AWS standards, but if a new CVN toughness standard is developed for the WRCVN specimens, this material may be found to have appropriate CVN toughness.

5.3. Conclusion

The conclusion of this study is that the most appropriate way to qualify fillet weld procedures is with a WRCVN toughness test along with macroetch and hardness tests done on T specimens that simulate the planned welds exactly. The requirements for CVN toughness will need to be revised for the WRCVN specimen, and hardness standards will need to be developed.

APPENDIX

Derivation of Equation 2.1

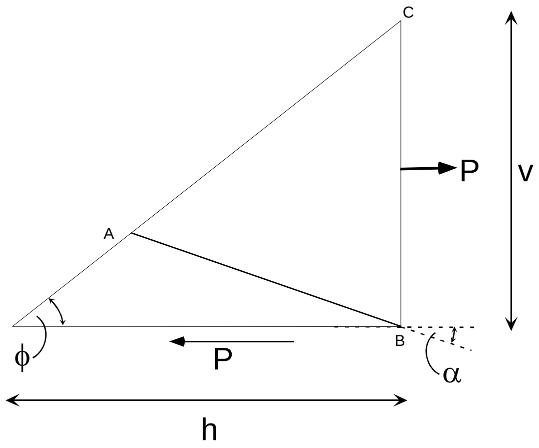

x = length $AB = h \sin \phi / \sin (\alpha + \phi)$

Equilibrium:

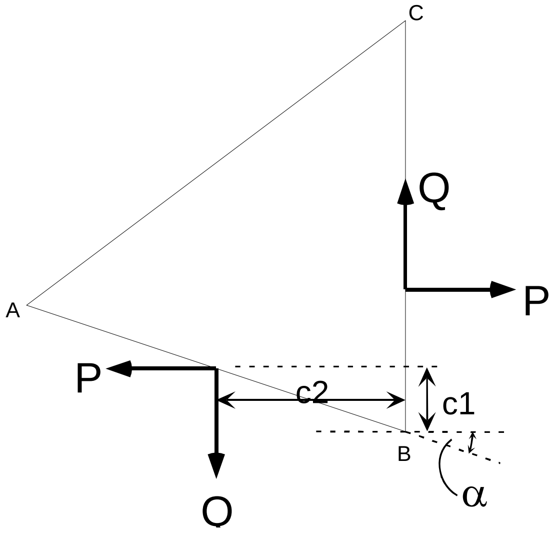
C
Q
P
A
P
c2
c1
B
α
O

$Q = (c1/c2)*P = aP \quad (a \equiv c1/c2)$

SHEAR FORCE:

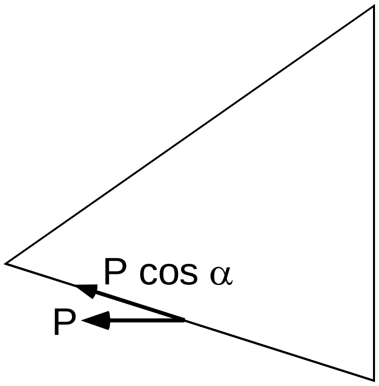

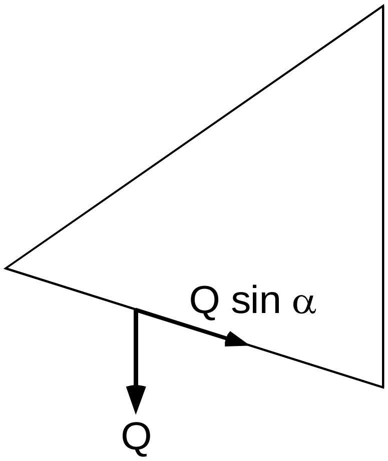

Q sin α = a * P sin α

Force = P cos α - a*P sin α = P(cosα - a sin α)

$$\tau = \frac{\text{force}}{A} = \frac{\text{force}}{Lx} = \frac{P(\cos\alpha - a\sin\alpha)}{Lh\sin\phi / \sin(\alpha+\phi)}$$

BIBLIOGRAPHY

AISC, 1995. *Manual of Steel Construction: Load and Resistance Factor Design*, 2nd ed. American Institute of Steel Construction.

AWS, 1992. Standard methods for mechanical testing of welds. ANSI/AWS B4.0-92, American Welding Society, Miami, FL.

AWS, 1996. *Bridge Welding Code*. ANSI/AWS D1.5-96, American Welding Society, Miami, FL.

ASTM, 1994. Standard methods and definitions for mechanical testing of steel products. ASTM A370-94, American Society for Testing and Materials, Philadelphia, PA.

Devore, J. and Peck, R, 1993. Statistics: *The Exploration and Analysis of Data*, 2nd. ed. Duxbury Press, Belmont, CA.

Hahin, C., 1990. Development of an as-welded notch impact toughness test for steel weldments. Submitted to Welding Journal July 1990.

Miazga, G. and Kennedy, D., 1988. Behavior of fillet welds as a function of the angle of loading. *Canadian Journal of Civil Engineering,* **16**: 585-599.

Miller, D., 1997. Thicker steel permits the use of opposing arcs. *Welding Inovation,* **XIV**(2): 7-8.

Salmon, C. and Johnson, J, 1996. *Steel Structures: Design and Behavior, Emphasizing Load and Resistance Factor Design,* 4th ed. Harper Collins, NY.